Calhoun
Institutional Archive of the Naval Postgraduate School

Calhoun: The NPS Institutional Archive

DSpace Repository

Theses and Dissertations 1. Thesis and Dissertation Collection, all items

1959

Magnetic field effects on critical currents in thin superconducting indium films

Holmes, Robert C.; Basso, Robert J.

http://hdl.handle.net/10945/14391

Downloaded from NPS Archive: Calhoun

DUDLEY KNOX LIBRARY

Calhoun is the Naval Postgraduate School's public access digital repository for research materials and institutional publications created by the NPS community. Calhoun is named for Professor of Mathematics Guy K. Calhoun, NPS's first appointed -- and published -- scholarly author.

Dudley Knox Library / Naval Postgraduate School
411 Dyer Road / 1 University Circle
Monterey, California USA 93943

http://www.nps.edu/library

NPS ARCHIVE
1959
HOLMES, R.

MAGNETIC FIELD EFFECTS ON CRITICAL CURRENTS IN THIN SUPERCONDUCTING INDIUM FILMS

ROBERT C. HOLMES
ROBERT J. BASSO

MAGNETIC FIELD EFFECTS ON CRITICAL CURRENTS IN THIN SUPERCONDUCTING INDIUM FILMS

* * * * * * *

Robert C. Holmes

and

Robert J. Basso

MAGNETIC FIELD EFFECTS ON CRITICAL CURRENTS IN THIN SUPERCONDUCTING INDIUM FILMS

by

Robert C. Holmes
Lieutenant Commander, United States Navy

and

Robert J. Basso
Lieutenant, United States Navy

Submitted in partial fulfillment of
the requirements for the degree of

MASTER OF SCIENCE

IN

PHYSICS

United States Naval Postgraduate School
Monterey, California

1 9 5 9

Thesis

959

OLMES, P.

MAGNETIC FIELD EFFECTS ON CRITICAL CURRENTS IN THIN SUPERCONDUCTING INDIUM FILMS

by

Robert C. Holmes

and

Robert J. Basso

This work is accepted as fulfilling
the thesis requirements for the degree of
MASTER OF SCIENCE
IN
PHYSICS
from the
United States Naval Postgraduate School

ABSTRACT

This project was undertaken in an effort to determine the effect of magnetic field on critical current in thin superconducting indium films. For this purpose films ranging in width from 0.003 centimeters to 0.012 centimeters and in thickness from 0.000006 centimeters to .00002 centimeters were utilized. The critical currents for these films were determined in the temperature range from 1.8° K to 3.4° K, in magnetic fields ranging from zero to 550 gauss, and for orientations (1) plane of film normal to the magnetic field, (2) long axis of the film parallel to the magnetic field and (3) short axis of the film parallel to the magnetic field.

It was found that the critical current is dependent on not only the strength of the magnetic field but also the orientation of the specimen within this field. Furthermore, it was found that the magnetic field has the greatest effect when the specimen is oriented normal to the field and the least effect when the specimen is oriented with its short axis parallel to the field.

TABLE OF CONTENTS

Section Title Page

1. Introduction 1

2. Theoretical Behavior of a Macroscopic Superconductor 5

3. Penetration Effects 13

4. Demagnetizing Currents in Thin Superconductors of Rectangular Cross Section 22

5. Current Behavior within a Superconductor as Critical Current Densities are Obtained 25

6. Possible Combined Effects of an Externally Applied Magnetic Field and a Conduction Current 28

7. Procedure of the Experiment 33

8. Experimental Results 35

9. Conclusions 37

10. Bibliography 55

Appendices

I. Proof of the Cooper Solution to the London Equation 56

II. Tables of Data 58

1. Introduction

The phenomenon of superconductivity is one which has eluded explanation for nearly half a century. Ever since Kamerlingh Onnes in 1911, while experimenting with mercury conductors, found to his astonishment that at very low temperatures the resistance did not just decrease gradually but rather suddenly and unexplainably fell to a value so nearly zero that it defied measurement, investigators have been steadily experimenting with a wide variety of substances in an attempt to gain further insight into this strange and unusual phenomenon. By using the most sensitive methods of resistance measurement known to date, it has been established that the resistivity of a superconductor is either truly zero or at least less than 10^{-20} ohm-cm.

As one might expect, it was not long after the discovery of superconductivity that attempts to apply Maxwell's equations to the superconducting state were made. On the basis of the Maxwellian relations, predictions were made concerning the probable behavior of a superconductor by simply assuming an infinite conductivity to exist. This "perfect" conductor treatment was widely accepted until in 1933, twenty-two years after the discovery of superconductivity, Meissner and Ochsenfeld undertook to investigate more fully the magnetic properties of a superconductor. The results of this investigation brought further

consternation to the theorist. The perfect conductor predictions were found to be invalid in the light of these experiments. Where the Maxwellian relations had predicted a "frozen in" field, there was in reality no field. It was found that a metal, upon passing into the superconducting state, seemingly expelled any existing field from within itself. Furthermore, application of Maxwell's equations to these new data led immediately to the undeniable fact that the current at depth in a superconductor must also be zero and therefore any superconducting current would have to flow as a surface current alone.

Thus, the first magnetic behavior experiments led to the abandonment of the strictly "perfect" conductor approach to superconductivity and added the necessary initial condition that the magnetic induction within a superconductor goes to zero along with the resistance[1]. It was therefore again possible to apply Maxwell's relations to the experimental facts which were (1) zero resistance and (2) zero magnetic induction. The pre-

---

[1] The phenomenon whereby a superconductor exhibits zero magnetic induction is given the name of Meissner effect. It was later shown that the existence of zero magnetic induction, while certainly true deep within a superconductor, is not ture at the surface where a definite penetration effect does exist.

dictions based upon these two initial conditions were then found to be valid in the case of macroscopic conductors.

Further investigation of the magnetic and electrical properties of superconductors on a more microscopic scale led to the discovery that, although very slight, the magnetic field does penetrate into the superconductor. When dealing with macroscopic conductors, the penetration depth is so slight as to be negligible; however, when considering thin wires and films this penetration depth is no longer negligible when contrasted with the dimensions of the conductor itself.

At about the same time as the above experiments were being performed, the incompatability of the strictly surface current predictions with the known behavior of conduction electrons[1] was causing disconcertion to some few individuals. Becker, Heller and Sauter, through consideration of charge and inertia of electrons, showed that the current and accompanying magnetic field should penetrate to a depth of approximately 10^{-5} cm. Shortly thereafter the F. and H. Londons advanced this theory by simply applying the new found experimental facts for a superconductor, i.e. at $x = 0$, $H = H$; and at $x = \infty$, $H = 0$.

---

[1] Because charge is not a homogeneous fluid, it was reasoned that the magnetic field must penetrate to a certain extent within the superconductor.

The generalization brought about by this seemingly simple application of initial conditions, has led to a quite complex set of predictions concerning such things as current distributions, kinetic energy of conduction currents, effects of moving conductors, alternating current behavior, etc. Possibly even more important, the theory of the Londons, together with two more recent theories, one by Heisenberg and another by Born and Cheng, has been instrumental in establishing superconductivity as a lattice phenomenon. Born and Cheng have shown a direct relation between the lattice structure of elements and the occurence of superconductivity.

It was no great length of time after the discovery of superconductivity that a very practical application of this new phenomenon suggested itself, that of a powerful, loss free, electromagnet. However, to the dismay of the eager experimenters, it was found that any time a superconductor was subjected to (1) a current greater than a certain critical current or (2) a magnetic field greater than a given threshold field, the superconducting specimen was found to switch back to the resistive state. It is the interaction of these above two phenomenon with which this project is concerned. The data assimilated in these pages deals directly with the effects of varying magnetic field and specimen orientation on the critical DC current.

2. Theoretical Behavior of a Macroscopic Superconductor.

In attempting to become better aquainted with the behavior of a superconductor, it is considered useful to compare the behavior of a macroscopic conductor as (1) a normal conductor, (2) a "perfect" conductor and (3) a superconductor. For a simplified study of magnetic effects it is often quite advantageous to utilize a ring with a toroidal winding since the magnetic field within the winding is confined to the space within the ring. Accordingly, such a specimen[1] will be used in this discussion.

2.1. Magnetic Behavior of a Normal Conductor

Consider a normal circular conductor as shown in Fig. 1. The winding A around the specimen is called the magnetizing winding and the current in the winding, the magnetizing current. Connected to the magnetizing winding is a source of potential controlled by a switch S as shown. The magnetic behavior within the

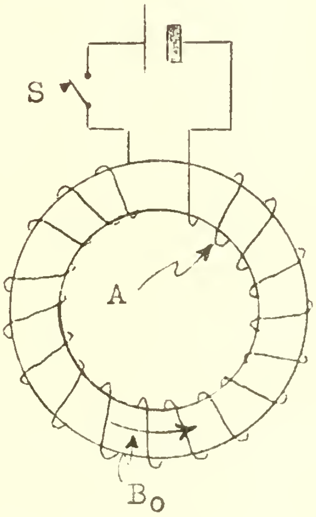

Fig. 1

---

[1] A specimen such as this is called a Rowland ring. It is named after J. H. Rowland who made use of such a ring in his experimental work.

2. Theoretical Behavior of a Macroscopic Superconductor.

In attempting to become better aquainted with the behavior of a superconductor, it is considered useful to compare the behavior of a macroscopic conductor as (1) a normal conductor, (2) a "perfect" conductor and (3) a superconductor. For a simplified study of magnetic effects it is often quite advantageous to utilize a ring with a toroidal winding since the magnetic field within the winding is confined to the space within the ring. Accordingly, such a specimen[1] will be used in this discussion.

2.1. Magnetic Behavior of a Normal Conductor

Consider a normal circular conductor as shown in Fig. 1. The winding A around the specimen is called the magnetizing winding and the current in the winding, the magnetizing current. Connected to the magnetizing winding is a source of potential controlled by a switch S as shown. The magnetic behavior within the

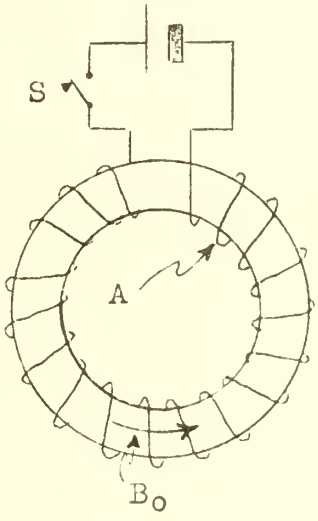

Fig. 1

---

[1] A specimen such as this is called a Rowland ring. It is named after J. H. Rowland who made use of such a ring in his experimental work.

specimen when the switch S is closed can be explained by basic electromagnetics in the following manner. Upon closing switch S a magnetizing current builds up in the magnetizing winding A. This build of current in A induces the build-up of a magnetic field within the specimen. However, as this magnetic field builds, it induces eddy currents within the specimen which in turn give rise to a secondary magnetic field which, at first, exactly counters the primary field induced by the magnetizing current. Due to the resistance of the specimen, however, these induced eddy currents exponentially drop to zero and the energy of the secondary field is quickly lost in resistive heating. Thus the total behavior of the magnetic field within the conductor may be shown graphically as in Fig. 2.

Now, let us hold all conditions as they are -- the switch S closed and the magnetic induction within the specimen at a steady state value of B_o. Now, if in addition to winding A we were to add another magnetizing winding C and another controlling

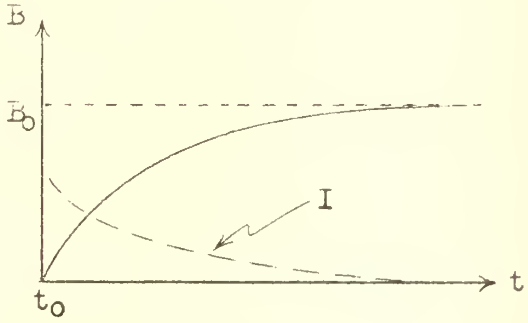

Fig. 2

B is the total magnetic induction within the conductor and I is the induced current. B_o is the steady state value of magnetic induction.

switch S' as shown in Fig. 3, we would find that upon closing switch S' at a time t_1, the time behavior of the total magnetic induction within the specimen would be as shown in Fig. 4. That is, the initial value of magnetic induction B_o would be exponentially increased to $B_o + B'$ upon closing the switch S'

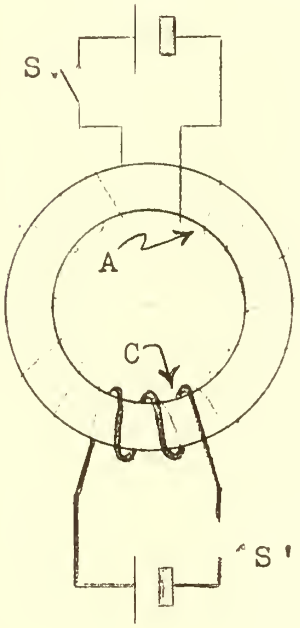

Fig. 3

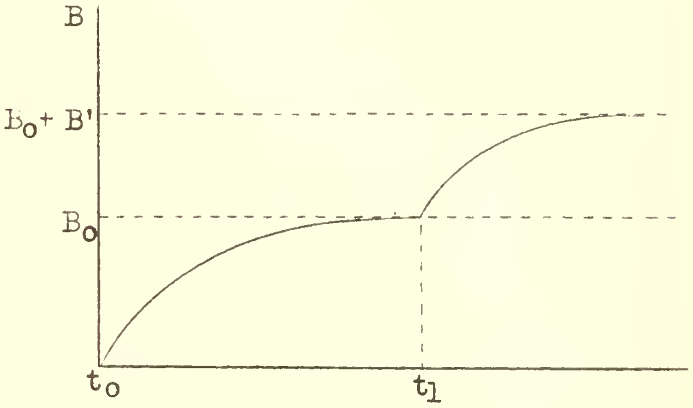

Fig. 4

The time behavior of the total magnetic induction.

2.2. Magnetic Behavior of a Perfect Conductor.

The differential form of Faraday's law states

$$\text{curl } \bar{E} = -\frac{\partial \bar{B}}{\partial t} \qquad (2.1)$$

In the case of a perfect conductor we have the additional relation that $R = 0$. This condition requires, from Ohms law, that $\bar{E} = 0$. Combining the zero electric field requirement with Faraday's law, one finds

$$\frac{\partial \bar{B}}{\partial t} = 0 \qquad (2.2)$$

which upon integration leads to

$$\bar{B} = \bar{B}_0 \qquad (2.3)$$

where $\bar{B}_0$ is the constant of integration.

Thus we find that Faraday's law, applied in the case of a "perfect" conductor, predicts that whatever magnetic induction was present in the specimen at the time it became "perfectly" conducting will become "frozen in" and cannot be changed by any means so long as the specimen remains in its "perfectly" conducting state. This result can be easily predicted from basic electromagnetic considerations as used in the example with the normal conductor. Reconsider the normal conductor situation in which the switch S̲ was closed and the magnetic induction within the specimen was stabilized at $\bar{B}_0$. For the present we will leave switch S̲' open so that no magnetizing current flows in coil C̲. Now, let us imagine that by some means we suddenly convert our specimen from a normal conductor to a "perfect" conductor with all other conditions remaining constant. Since the specimen is in a steady state condition wherein there are no currents flowing within the specimen and no changing fields to induce any current flow within the specimen, to all outward appearances we would expect all to remain as is, that is, the same current should continue to flow in coil

A and the same amount of magnetic induction should exist within the ring. Now, however, let us open the switch S and predict the results. When S is opened and the magnetization current starts to fall, the induced field within the perfect conductor should likewise start to collapse and in doing so should induce currents on the specimen which, by Lenz's law, would tend to maintain the field at its original value. In the case of the normal conductor we have seen that these currents would rapidly decay due to the resistance of the specimen; however, in the case of a "perfect" conductor with zero resistance, the currents would not die out but should continue to flow in such a manner as to maintain the magnitude of the magnetic induction within the specimen at a constant level.[1] Now, since we have no current flowing within winding A, we may remove this winding without effecting the specimen in any manner.

Again, in a like manner, if we close the switch S', the current would rise in coil C but no increased magnetic induction would appear since as the field within the ring tries to build, it again induces non-decaying currents on the specimen which flow in such a manner as to maintain the field at a constant level.

---

[1] It will later be shown that the magnetic induction within a superconductor is constant at zero. That is, $\bar{B}_0 = 0$.

Although the preceeding argument presents a gross oversimplification of the induction equation, it does serve to present an easily understandable picture of the anticipated behavior of a "perfect" conductor. One should realize, however, that there is, in reality, no primary or secondary field but simply a total field. Had this field been induced by the winding A when the specimen was in the normal state, and had the specimen subsequently become perfectly conducting, then when the switch S was opened one would have expected to observe no change at all in the total magnetic induction but simply a jumping of the current from coil A to the surface of the ring. That is, one would expect a more or less mirror current to appear on the specimen and flow so as to exactly oppose any attempted disturbance of the field within the conductor.

We have, by basic electromagnetic considerations, shown logically the result predicted by the induction equation for the case of a "perfect" conductor. Similiar arguments could be presented to show the current behavior within a "perfect" conductor which one can predict from the equation

$$\text{curl } \bar{H} = \bar{J} \; . \qquad (2.4)$$

Since $\bar{H}$ has been predicted to be constant within a perfect conductor, it follows from Eq. (2.4) that $\bar{J}$ is also predicted to be a constant, $\bar{J}$ is then

$$\bar{J} = \bar{J}_0 \qquad (2.5)$$

At first glance Eq. (2.5) appears contradictory to our previous prediction of a "mirror" current however this is quite easily resolved as follows. From Eq. (2.4) it can be shown that if a discontinuity exists in $\bar{H}$, then a surface current flows whose current density is equal to the cross product of the surface discontinuity in H by the unit normal to the surface or

$$\bar{J}' = (\bar{H}_e - \bar{H}_0) \times \hat{n} \qquad (2.6)$$

where $\bar{J}'$ is the surface current density, $\bar{H}_e$ is the external field, $\bar{H}_0$ is the field within the perfect conductor and $\hat{n}$ is the outer unit normal to the surface.

The above relations predict that the previously anticipated mirror currents and any other currents which are passed through any perfect conductor must travel as surface currents; furthermore, they are not merely predicted to flow near the surface but actually at the surface and exactly along the surface of discontinuity[1].

2.3. Magnetic Behavior of an Actual Superconductor.

Following the discovery of the phenomenon of superconductivity, for a period of twenty-two years, it was generally accepted that the previously stated predictions

---

[1] The concept of current flow exactly at the surface of discontinuity was later shown by Becker, Heller and Sauter, and the F. and H. Londons, to be inconsistent with established properties of conduction electrons.

concerning the behavior of a perfect conductor applied to the superconducting state. It was not until 1933 that Meissner demonstrated the contrary. His experiments showed that the magnetic field, instead of being "frozen in", was forceably expelled from the superconductor at the time the superconducting state appeared[1]. This discovery provided a second condition of the superconducting state, that of zero magnetic induction[2].

This condition requires a departure from the perfect conductor approach in that the integration constants of Eq. (2.3) and (2.5) have been experimentally determined to be zero. This leads to the new relations

$$\bar{B}_0 = 0 \tag{2.7}$$

$$\bar{J}_0 = 0 \tag{2.8}$$

$$\bar{J}' = \bar{H}_e \times \hat{n} \ . \tag{2.9}$$

Thus, at the time the specimen becomes superconducting, the field is expelled from within the superconductor. Then, any further attempts to alter the field within the

---

[1] The condition of zero magnetic induction was later shown to be only partially true. A small penetration of field does exist within the superconductor but does not become evident except in experiments on a more microscopic scale.

[2] In early writing the superconducting state was often defined by (1) zero resistance and (2) zero magnetic induction. After the discovery of penetration effects, this defining condition could no longer be used.

specimen will, as before, result in "mirror" currents which act in such a manner as to retain the field within the specimen at a zero level.

Consider again the ring shown in Fig. 1. Let us assume the ring is in the superconducting state and the switch S is open. If we now close the switch S a magnetizing current will build in winding A. As this current builds it induces a field within the specimen. This field, in turn, induces currents on the surface of the conductor in such a manner that a counter field is formed exactly equal and opposite to the primary field. Thus, the net effect of closing the switch S upon the zero field within the superconductor is that it has no effect at all. Whenever a condition is established which would cause a field inside the superconductor, its very establishment provides the motivating force for the "mirror" current which acts so as to exactly cancel its effects within the superconductor. This mirror current will hereafter be refered to as the demagnetization current.

3. Penetration Effects.

The equations of the section were based upon two phenomenon observed in macroscopic superconductors, (1) zero resistance and (2) zero magnetic induction. It has been shown that a consequence of the above conditions was a prediction that current flow in a superconductor

is a surface phenomenon; moreover, such a treatment requires that the surface current flow in a region of discontinuity, a zero thickness surface at the boundary of the superconductor. Two groups of investigators, Becker, Heller and Sauter, and F. and H. Londons, maintained the concept of the flow of charge over a surface of zero thickness was not consistent with the characteristics of charge flow obtained from either classical or quantum mechanical considerations, i.e., the flow of charge by electron transfer requires more than a two dimensional surface.

In the year 1933, the penetration effects of the magnetic field were definitely shown to be plausible by a theory by Becker, Heller and Sauter who approached the phenomenon of superconductivity from a consideration of charge and inertia of conduction electrons. Although their theory came at approximately the same time as Meissner's discovery of zero magnetic induction within a superconductor of macroscopic dimension, a concept which their theory did not encompass, it did serve to provide the groundwork for a later theory by the Londons in 1935. This refinement by the Londons led to what has come to be known as the London equation, an equation which does contain the fact of zero magnetic induction observed in macroscopic superconductors.

3.1. The London Equation.

If an electron were subjected to an electric field, $\bar{E}$, and if such an electron were also experiencing zero resistance to its movement, a force equation could be written as

$$m\,\dot{\bar{v}} = \bar{E}\,e \,, \qquad (3.1)$$

where m is the mass of the electron, $\dot{\bar{v}}$ is its accelleration and e its charge. Solving for $\bar{E}$ one obtains

$$\bar{E} = \frac{m\,\dot{\bar{v}}}{e} \,. \qquad (3.2)$$

Now, Eq. (3.2) will remain unchanged if one performs the following unity multiplications;

$$\bar{E} = \frac{m\,\dot{\bar{v}}}{e}\left(\frac{e}{e}\right)\cdot\left(\frac{n}{n}\right)\left(\frac{\mu_o}{\mu_o}\right) , \qquad (3.3)$$

where μ_o is the permeability of free space and n is the number of electrons per unit volume. If one now calls

$$\lambda^2 = \frac{m}{\mu_o n e^2}$$

we may write Eq. (3.3) as

$$\bar{E} = \mu_o \lambda^2 (n\,e\,\dot{\bar{v}}) \,. \qquad (3.4)$$

Recalling the expression for current density $\bar{J}$ to be

$$\bar{J} = n\,e\,\bar{v} \,, \qquad (3.5)$$

one can determine the time rate of change of current density to be

$$\dot{\bar{J}} = n\,e\,\dot{\bar{v}} \,. \qquad (3.6)$$

One may thus write for $\bar{E}$

$$\bar{E} = \mu_o \lambda^2 \dot{\bar{J}} \,. \qquad (3.7)$$

Now, taking the curl of both sides of Eq. (3.7)

$$\text{curl } \bar{E} = \mu_0 \lambda^2 \text{curl } \dot{\bar{J}} \qquad (3.8)$$

but from Maxwell's equations

$$\text{curl } \bar{E} = -\mu_0 \dot{\bar{H}} \qquad (3.9)$$

within a substance with zero magnetization. Substitution of Eq. (3.9) in Eq. (3.8) yields, therefore,

$$-\mu_0 \dot{\bar{H}} = \mu_0 \lambda^2 \text{curl } \dot{\bar{J}}$$

or

$$-\dot{\bar{H}} = \lambda^2 \text{curl } \dot{\bar{J}} \ . \qquad (3.10)$$

Again, from Maxwell's relations,

$$\text{curl } \dot{\bar{H}} = \dot{\bar{J}} \ ; \qquad (3.11)$$

taking the curl of each side of Eq. (3.11) one obtains by assuming $\nabla \cdot \dot{\bar{H}} = 0$

$$-\nabla^2 \dot{\bar{H}} = \text{curl } \dot{\bar{J}} \qquad (3.12)$$

and substitution of Eq. (3.12) into Eq. (3.10) gives us

$$\nabla^2 \dot{\bar{H}} = \frac{\dot{\bar{H}}}{\lambda^2} \ . \qquad (3.13)$$

Integrating Eq. (3.13) with respect to time one finds

$$\nabla^2 (\bar{H} - \bar{H}_0) = \frac{(\bar{H} - \bar{H}_0)}{\lambda^2} \qquad (3.14)$$

which was the Becker, Heller and Sauter equation. The Londons modified this equation however by noting that for macroscopic superconductors one may consider $\bar{H}_0 = 0$. This assumption leads to the London equation

$$\nabla^2 \bar{H} = \frac{\bar{H}}{\lambda^2} \qquad (3.15)$$

and the current equation

$$\nabla^2 \bar{J} = \frac{\bar{J}}{\lambda^2} \qquad (3.16)$$

3.2. Solutions to the London Equation.

As derived in Sec. 3.1., the London equation has the form

$$\nabla^2 \bar{H} = \frac{\bar{H}}{\lambda^2}$$

Writing this out in its cartesian components one obtains

$$\frac{\partial^2 \bar{H}}{\partial x^2} + \frac{\partial^2 \bar{H}}{\partial y^2} + \frac{\partial^2 \bar{H}}{\partial z^2} = \frac{H_x \hat{i} + H_y \hat{j} + H_z \hat{k}}{\lambda^2} \quad . \quad (3.17)$$

If one assumes the value of H to be dependent on the depth within the superconductor only, the following solutions are of interest.

3.2.1. Infinite Wall Solution.

If one considers the penetration effects of a magnetic field, as given by the London equation, on an infinite wall as shown in Fig. 5, then Eq. (3.17) may be written as

$$\frac{d^2 \bar{H}}{dx^2} = \frac{\bar{H}}{\lambda^2} \ .$$

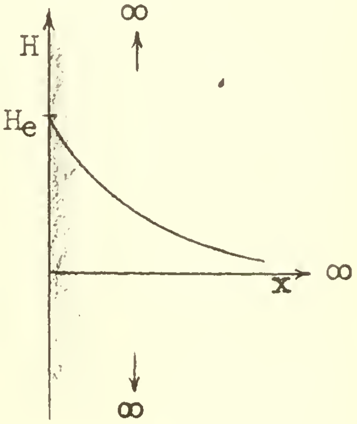

Fig. 5

The solution to this equation takes the form

$$\bar{H} = \bar{C}_1 e^{\frac{1}{\lambda}x} + \bar{C}_2 e^{-\frac{1}{\lambda}x}$$

where $\bar{C}_1$ and $\bar{C}_2$ are arbitrary constants of integration. To evaluate these constants we make use of two initial conditions; $\bar{H} = \bar{H}_e$ at $x = 0$ and $\bar{H} = 0$ at $x = \infty$. H_e is the field at the external surface of the superconductor. From the first condition one obtains the relation

$$\bar{C}_1 + \bar{C}_2 = H_e \ .$$

From condition (2) one finds

$$\bar{C}_1 = 0$$

Thus, we find that the solution to Londons' equation in the case of an infinite wall is

$$\bar{H} = \bar{H}_e \, e^{-\frac{1}{\lambda}x} \, . \tag{3.18}$$

A plot of $\bar{H}/\bar{H}_e$ is given in Fig. 6.

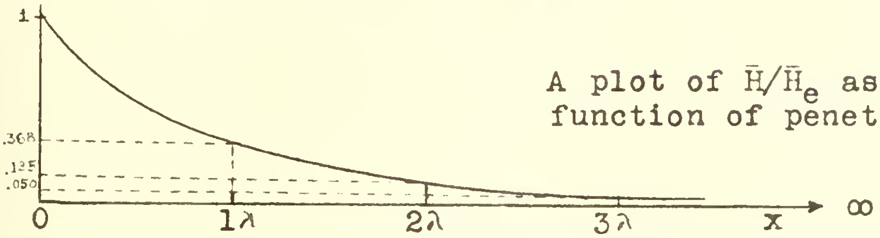

A plot of $\bar{H}/\bar{H}_e$ as a function of penetration.

Fig. 6

3.2.2. Superposition Solution for an Infinite Slab.

In the event a superconducting slab is under investigation, one can obtain an approximate solution to the London equation by means of the method of superposition providing the thickness of the slab is of the order of three or four lambda or more.

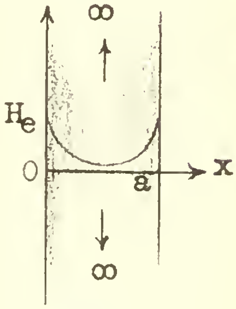

Fig. 7

By this method, the total H should be approximately equal to the sums of two infinite wall solutions as

$$\bar{H} = \bar{H}_1 + \bar{H}_2 \quad \text{or} \quad \bar{H} = \bar{H}_e \left(e^{-\frac{1}{\lambda}x} + e^{\frac{1}{\lambda}x} e^{-\frac{1}{\lambda}a} \right) \tag{3.19}$$

A plot of this equation is shown in Fig. 8 for a slab of four lambda thickness. A solution of this type could be easily applied to a superconductor with a rectangular cross section if, as before, the minimum dimension of the speci-

men were no less than three or four lambda.

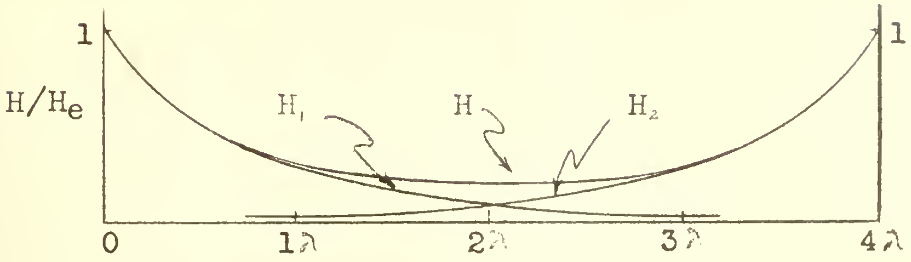

Fig. 8

3.2.3. The Exact Solution to the London Equation for an Infinite Slab.

It was shown in Sec. 3.2.1. that the solution to the London equation, in the case of a one dimensional variation, takes the form

$$\bar{H} = \bar{C}_1 e^{-\frac{1}{\lambda}x} + \bar{C}_2 e^{\frac{1}{\lambda}x} .$$

For a slab of thickness a, the following initial conditions apply;

$$(1)\ \bar{H} = \bar{H}_e \text{ at } x = 0$$

$$(2)\ \bar{H} = \bar{H}_e \text{ at } x = a .$$

From the first condition one obtains

$$\bar{C}_1 + \bar{C}_2 = \bar{H}_e$$

and from the second condition

$$\bar{C}_2 = \frac{(1 - e^{-\frac{a}{\lambda}})}{(e^{\frac{a}{\lambda}} - e^{-\frac{a}{\lambda}})}\bar{H}_e ,$$

from which

$$\bar{C}_1 = \frac{(e^{\frac{a}{\lambda}} - 1)}{(e^{\frac{a}{\lambda}} - e^{-\frac{a}{\lambda}})}\bar{H}_e .$$

Thus, the exact solution to the problem of the infinite slab becomes

$$\bar{H} = \frac{\bar{H}_e}{(e^{\frac{a}{\lambda}} - e^{-\frac{a}{\lambda}})}\left(e^{\frac{x}{\lambda}} - e^{-\frac{x}{\lambda}} + e^{\frac{a-x}{\lambda}} - e^{-\frac{a-x}{\lambda}}\right) \quad (3.20)$$

The exact values of H as obtained from Eq. (3.20) and the approximate values as obtained from Eq. (3.19) are presented in Table 1 for the case of an infinite slab of four lambda thickness.

Thickness	H/H_e approximate	H/H_e exact
0	1.018	1.000
1	0.416	0.410
2	0.271	0.268
3	0.416	0.410
4	1.018	1.000

Table 1

Due to the inaccuracies introduced through uncertainties in sample thickness and inaccuracies introduced by considering the sample to be perfectly rectangular in cross section, it is felt that the superposition solution will give sufficient accuracy for determining the field at any point within the superconductor. The approximate solution affords a considerable time saving especially in the case of the rectangular cross section.

3.2.4. The Exact Solution to the London Equation for an Infinitely Long Superconductor of Rectangular Cross Section.

A solution to the London equation for an infinitely long superconductor of rectangular cross section has been proposed by Dr. J. N. Cooper of the U. S. Naval Postgraduate School to be

$$\bar{H} = C\, e^{-\frac{a+b}{\sqrt{2}\lambda}} \left[\hat{i}\left(e^{+\frac{x}{\sqrt{2}\lambda}} + e^{-\frac{x}{\sqrt{2}\lambda}}\right)\left(e^{-\frac{y}{\sqrt{2}\lambda}} - e^{\frac{y}{\sqrt{2}\lambda}}\right) + \hat{j}\left(e^{\frac{x}{\sqrt{2}\lambda}} - e^{-\frac{x}{\sqrt{2}\lambda}}\right)\left(e^{\frac{y}{\sqrt{2}\lambda}} + e^{-\frac{y}{\sqrt{2}\lambda}}\right)\right] \quad (3.21)$$

where a and b are the dimensions shown in Fig. 9.

A proof that Eq. (3.21) does satisfy the London equation is offered in Appendix I.

A plot of $\bar{H}$ as a function of position may be made from Eq. (3.21) as shown in Fig. 10. This plot is made for a specimen of dimensions comparable to those utilized in this investigation.

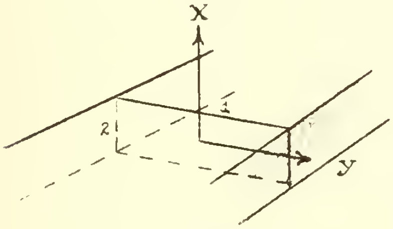

Fig. 9

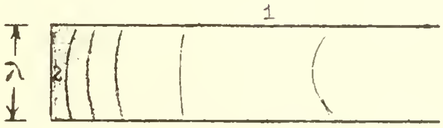

Fig. 10

It can be seen that the greater penetrations of magnetic field and the greater concentrations of magnetic field are predicted to occur at the edges of the specimen whenever a current is passed through it. Thus, one might conclude that whenever one passes a conduction current through a superconductor whose dimensions are comparable to those shown in Fig. 10, a rather high current density and penetration is to be expected along the edges whereas an extremely shallow penetration and lower current density should be anticipated on the top and the bottom surfaces. These current and field concentrations are shown in Fig. 10.

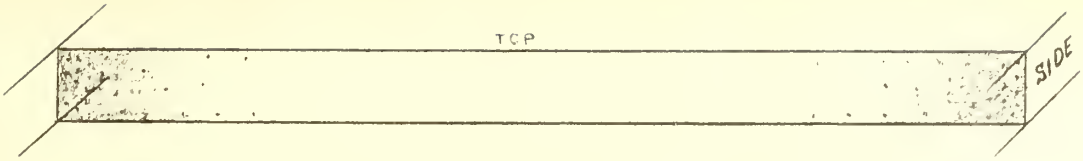

Fig. 11

Conduction Current distribution over a cross sectional element of a rectangular superconductor. Darker areas indicate loci of high current density.

4. Demagnetization currents in Thin Superconductors of Rectangular Cross Section.

It has been shown in Sec. 2 that whenever a superconductor is subjected to an external magnetic field, a current is caused to flow within the superconductor in such a way as to counter the effects of the applied field. This current is known as the demagnetizing current. The macroscopic treatment utilized in Sec. 2 neglected the penetration effects treated in Sec. 3. One can, however, generalize the treatment of Sec. 3 to cover the case of the demagnetizing current as well as the conduction current through the specimen since Eq. (3.1) is equally applicable. It is thus useful to consider the demagnetization current densities which one might anticipate in various specimen orientations within an external field.

4.1. Demagnetization Current when Orientation is such that the Broad Plane of the Superconductor is Normal to the Applied Field.

Consider a superconductor whose thickness is of the

order of one lambda and whose width is several lambda or more[1]. Let the orientation of this sample, with respect to the applied magnetic field H, be as shown in Fig. 12a. With no externally applied field, no demagnetization current will flow; however, as soon as any finite value of external field is applied, a demagnetization current will appear. Since the superconductor considered has a thickness of the order of one lambda, one can reasonably assume a fairly uniform value of magnetic induction to exist from top to bottom of the specimen. One could thus assume a field distribution as shown in Fig. 12b and 12c and a current distribution as shown in Fig. 12d.

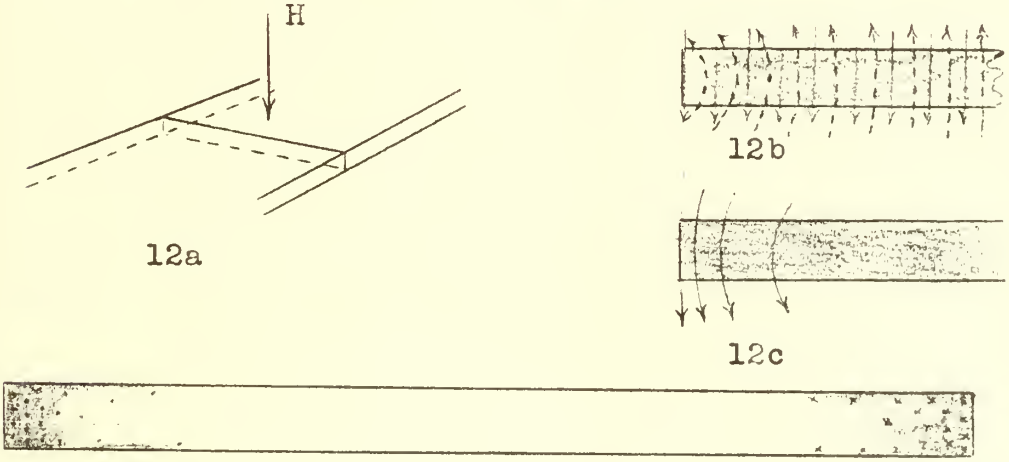

12a

12b

12c

12d

(Dots and crosses indicate direction of current)

Fig. 12

---

[1] This corresponds to the dimensions of the specimens investigated in this project.

It should be noted that the distributions shown in Fig. 12 are a consequence of

$$\nabla^2 \bar{H} = -\frac{\bar{H}}{\lambda^2}$$

$$R = 0$$

and

$$\text{curl } \bar{H} = \bar{J}$$

4.2. Demagnetization Current when Orientation is such that the Long Axis of the Superconductor is Parallel to the Applied Field.

By similiar reasoning to that applied in Sec. 2.3. and Sec. 4.1, one finds that the demagnetization field and current distributions for the orientation of Fig. 13a should be similiar to that shown in Fig. 13b and 13c.

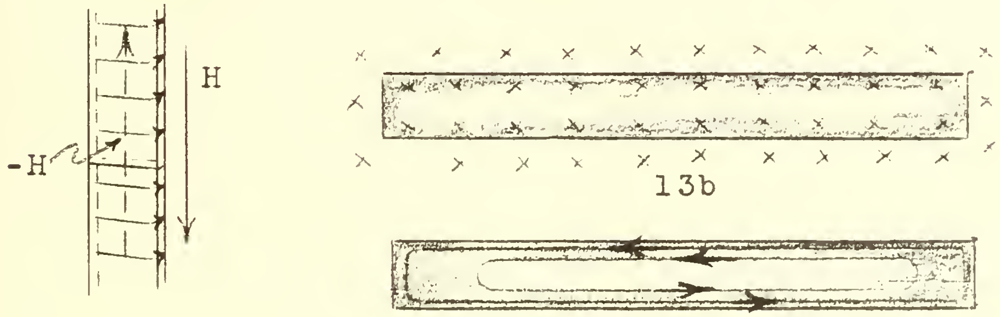

13b

13a

13c

Fig. 13

(a) Orientation in the externally applied magnetic field with arrows representing current.
(b) Magnetic field distribution looking down on a cross sectional area.
(c) Current distribution over a cross sectional area as viewed from above.

(Crosses indicate direction into plane of paper)

4.3. Demagnetization Current when Orientation is such that the Short Axis of the Superconductor is parallel to the Magnetic Field.

For the orientation as shown in Fig. 14a similiar results as for the other two orientations are obtained as shown in Fig. 14b and 14c.

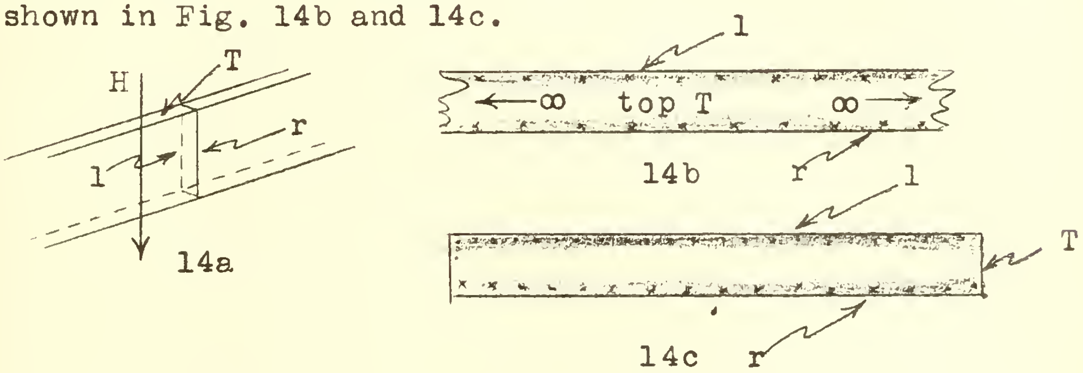

Fig. 14

(a) Specimen orientation
(b) Magnetic field distribution looking down on top T
(c) Demagnetization current distribution over a cross sectional area

5. Current Behavior within a Superconductor as Critical Current Densities are Obtained.

Thus far, in studying the current and field distributions within a thin superconductor, no mention has been made of the anticipated behavior as the current or magnetic field approach the critical values. It is obvious that, as the conduction current through a superconductor is increased or as the externally applied magnetic field is increased, critical current densities will soon be achieved at certain loci within the specimen. If one con-

siders the orientation as in Sec. 4.1. where the broad plane is normal to an externally applied field, one might anticipate the following sequence as the applied field is increased from zero to a critical value. First, one would, as previously discussed, anticipate a buildup of demagnetization current within the specimen as shown in Fig. 15b as the applied field is increased. Eventually, however, one would expect the edges to achieve their critical value of field and current. It may be reasoned that when this occurs, the portion of the specimen wherein the critical values exist either switch to some intermediate state or switch to an entirely resistive state. Since a switch to a purely resistive state in these regions would tend to indicate the existence of an oscillatory current[1], a fact for which no experimental verification exists, it will be assumed that the switch does occur via an intermediate state. If no oscillatory effects are to be hypothesized, one might conclude that the current in an intermediate state remains at the critical value and experiences no further buildup until all pure superconducting paths have

---

[1] It can be reasoned that if the switch occured to the purely resistive state, then the current would jump from the resistive area to a superconducting area. When this would occur, however, the resistive area would find itself without the critical value of current and would thus switch back to a superconducting state whereupon the current would reenter the area causing the cycle to repeat.

achieved the critical value of current density. One might thus expect an increase in the externally applied magnetic field to result in an inward movement of the demagnetization current until, at last, at a given value of the applied field, the entire specimen should be in the intermediate state. Further increase in field beyond this point could then be expected to result in a complete switch to the resistive state. This sequence of events is shown in Fig. 15.

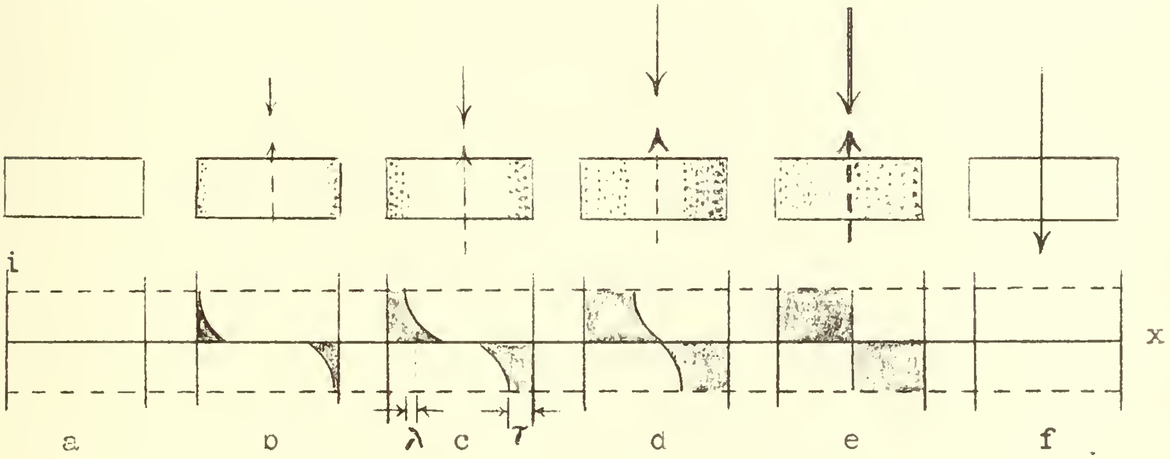

Fig. 15

Demagnetization Current as a Function of Depth from Edge

(a) Superconducting with no applied field.
(b) Demagnetizing current and field start to counter the applied field.
(c) Intermediate zone $\underline{\tau}$ begins to appear.
(d) Intermediate zone $\underline{\tau}$ spreads.
(e) Entire specimen in intermediate state.
(f) Final increase in applied field drives the entire specimen resistive.

Note: A current vs. position plot is shown under each state. The broken lines indicate critical currents.

The same type of approach to the concept of the intermediate state can be made for the conduction current. The same type of plots could be made for that case as in Fig. 15; the only difference being in the direction of flow for half the diagram. With conduction current, the current on either side would be plotted in the same direction.

6. Possible Combined Effects of an Externally Applied Magnetic Field and a Conduction Current.

We have considered in Sec. 3 and 4 the anticipated distribution of current[1] and field whenever a conduction current or an external magnetic field is independently applied to a thin rectangular superconducting specimen. Section 5 presented a possible behavior of current distribution whenever critical values of current and field are obtained at certain points within the specimen. It may now be helpful to consider possible combined effects when conduction current and external field are applied in combination and with sufficient magnitude to induce the intermediate state within the specimen.

Figure 16 presents the three orientations studied in this investigation and the hypothesized current and field distributions due to the externally applied magnetic field.

---

[1] Note that these distributions of current are based on the fact that there is symetry along the z axis. If this assumption is not true, the anticipated distributions would be altered.

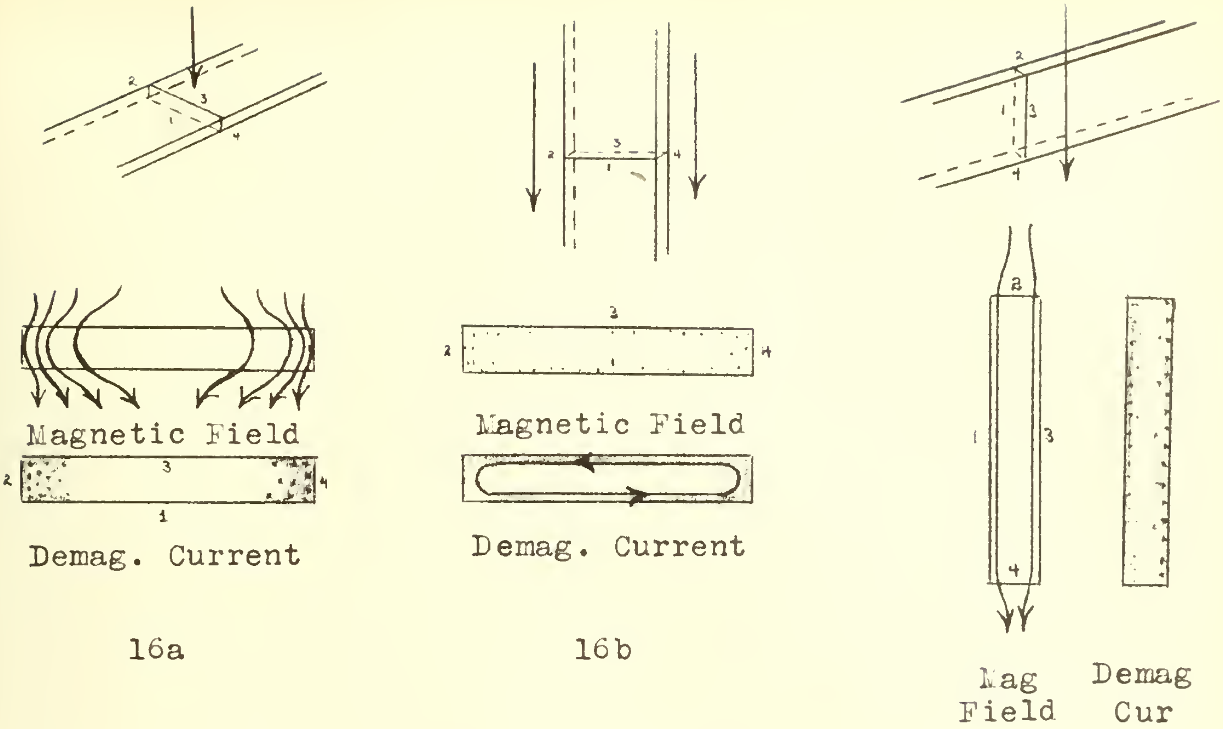

16a

16b

16c

Fig. 16

Fig. 17 presents the conduction current distribution as determined in Sec. 3.2.4.

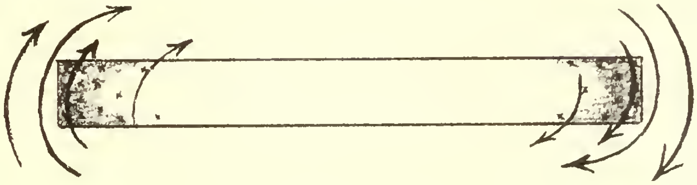

Fig. 17

Note that by superimposing the conduction current distribution of Fig. 17 on the demagnetization current distributions of Fig. 16a, 16b and 16c, one finds that in the orientations of 16a and 16c we have two points of interest. First, in each of these cases we have

conduction current flowing in regions wherein London's equation appears to predict external magnetic field penetration. If this observation is true, then the initial force equation from which the London equation was derived,

$$m\,\dot{\bar{v}} = \bar{E}\,e \;, \tag{6.1}$$

appears to have been incomplete since the total force on a moving electron in an electric and a magnetic field is

$$m\,\dot{\bar{v}} = e(\bar{E} + \bar{v} \times \bar{B}) \;. \tag{6.2}$$

Second, again superimposing the conduction current of Fig. 17 on Fig. 16b and Fig. 16c, one finds that a possible cancellation effect may very likely exist since in a portion of the specimen on finds the conduction current flowing so as to reinforce the demagnetization current; but in another part of the specimen one finds the conduction current acting in opposition to the demagnetization current. If this cancellation and addition effect exists, and there is no reason to believe it does not, then we must surely expect to find a large degree of asymmetry in these two orientations whenever a conduction current and an external field are present together. Figures 18a, 18b and 18c present a purely speculative hypothesis as to a possible current and field distribution for the three orientations of Figs. 16a, 16b and 16c when a conduction current is flowing through a specimen subjected to an external magnetic field. Note that in the orientation of Fig. 18a we have a very unsymmetrical pattern of

both the penetrating field and the conduction and demagnetization current. However, note also that in this orientation one would expect very little, if any, increase in total current flowing through the specimen due to the cancellation effect which might be anticipated.

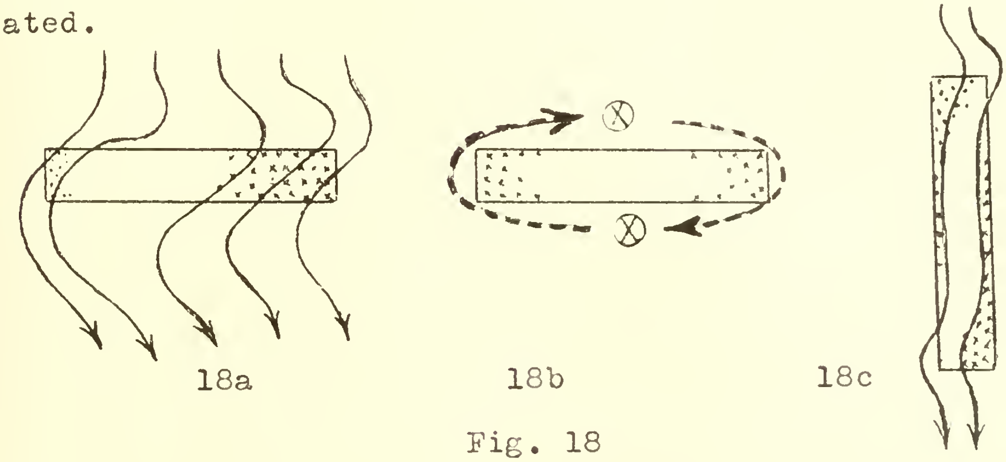

18a 18b 18c

Fig. 18

In the orientation of Fig. 18b, the broken line external to the specimen represents the field due to the conduction current while the circled cross indicates the direction of the applied field. The crosses within the specimen represent conduction current whereas the broken line inside the specimen represents the demagnetization current. Note that in this case one finds the demagnetization current acting in quadrature with the conduction current. In this orientation we would thus expect no cancellation effects. Whether additive effects exist is a purely speculative question which only experimentation can answer at the present state of knowledge. One should also note that the predicted straight paths

for the conduction electrons in this orientation holds true only for those electrons entering the specimen exactly parallel to the penetrating external field. Any entering at some angle with these field lines would likely have some sort of a distorted spiral path around the lines as they pass through the specimen.

The orientation of Fig. 18c exhibits the anticipated cancellation effects with slight distortion of magnetic field and current distribution. One would expect a rather slight effect on the switching characteristics in this orientation.

If one considers the areas about which the demagnetization current must flow in the various orientations, one finds that in the orientation of Fig. 18a the current must flow around a rather large area with respect to the other two orientations. Since the intensity of the field within such a pattern is directly related to the dimensions of the pattern, one finds that a large demagnetization current will be required in this orientation in order to cancel the applied field within the specimen.

In the orientations of Figs. 18b and 18c one finds the area around which the demagnetization current must flow to be quite small. It is therefore anticipated that in these two orientations the demagnetization current will be quite low.

It should be remembered that the current and field distributions presented in this section are highly spec-

ulative and open to doubt. It is felt that an accurate and dependable solution would have to start at Eq. (6.2) from which a differential equation of the form of the Londons' might be found. A proper solution to such an equation would be required for an exact determination.

7. Procedure of the Experiment.

In order to gain further knowledge of the behavior of superconducting specimens such as those discussed in the previous pages, this project was arranged by Dr. E. C. Crittenden of the U. S. Naval Postgraduate School.

The specimens used in this investigation consisted of thin indium films evaporated onto optically polished glass and quartz. The specimens were placed in a holder equipped with the necessary electrical leads for measuring current flow through and voltage drop across the specimen. The holder was so constructed that it was possible to achieve the three orientations of Fig. 16 for each of the specimens utilized while such specimens were inserted in a liquid helium bath within a cryostat[1]. The open end of the cryostat was sealed to a brass mounting plate in which were constructed several pressure tight electrical couplings to which were connected the

---

[1] The cryostat used in this project consisted of a long glass tube sealed at the bottom end and provided with a double wall over the bottom half. The air was evacuated from within this double wall providing good thermal insulation.

coaxial electrical leads from the specimen. The brass plate was also equipped with connections for evacuating the cryostat by means of a vacuum pump, and a pressure tight cap for filling with liquid helium. The cryostat was surrounded by a jacket of liquid nitrogen in a Dewar flask which acted as a thermal insulator for the liquid helium. A set of water-cooled Helmholtz coils were mounted around the complete unit and the specimen was centered at the point of maximum flux. The magnetic field was controlled by means of a variable resistance network in series with the coils. The temperature was controlled with a vacuum pump and a pressure regulator, the temperature being a function of the reduced vapor pressure within the cryostat. The pressure was measured with a mercury manometer except at very low ranges where an oil manometer was employed to increase the accuracy. Electrically, the specimen was connected in series with a type 541 Tektronix oscilloscope and a current-regulating circuit designed by Dr. E. C. Crittenden. This circuit, when triggered, provided a steady increase of current through the specimen until the specimen switched into the resistive state whereupon the thyratron control was fired by a trigger impulse from the oscilloscope thereby opening the circuit and preventing possible destruction of the specimen by "burn out".

The oscilloscope was employed for a visual presentation of the voltage and current across the specimen.

8. Experimental Results.

The effect of magnetic field on critical current for thin superconducting indium films in the various orientations of Fig. 19 are shown graphically on pages 41 through 54. The tabulated findings are listed in Appendix II.

It was found that a magnetic field had the greatest effect when the specimen was oriented as shown in Fig. 19a and the least effect when oriented as shown in Fig. 19c. An intermediate effect, slightly greater than that obtained in the orientation of Fig. 19c, was observed for orientations as shown in Fig. 19b.

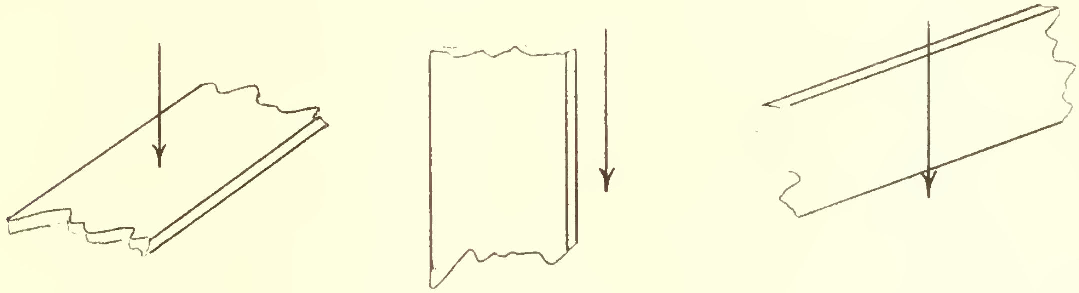

19a 19b 19c

Fig. 19

Specimen orientations in which the (a) greatest, (b) intermediate and (c) least effect of an externally applied magnetic field were observed.

The manner in which the magnetic field effects the critical current for any given orientation and temperature is presented graphically on pages 52 through 54 .

The effect of orientation in an externally applied magnetic field is summarized in Fig. 20

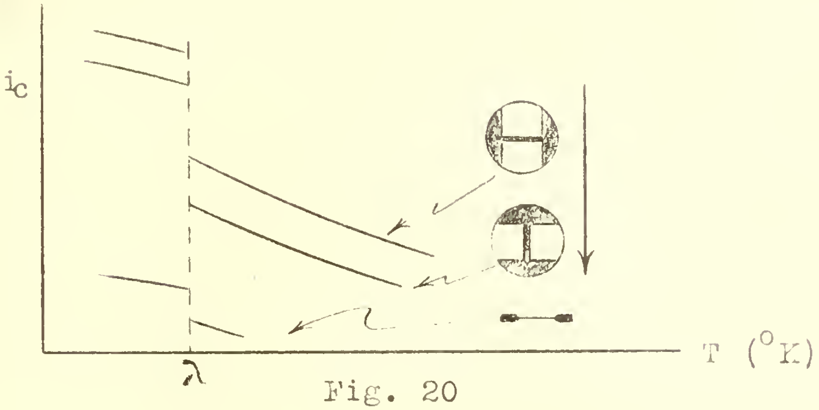

Fig. 20

The specimens utilized for the determinations in the orientation of Fig. 19a were Nos. 85, Q-8 and Q-9; the specimens utilized in the orientation of Fig. 19b were Nos. 100, 85, Q-8 and Q-9: and those utilized in the orientations of Fig. 19c were Nos. 85 and Q-8.

The dimensions of the specimens utilized in this project are listed in Table 2.

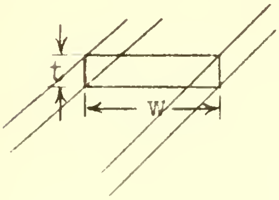

Specimen	width w	Thickness t
100	30μ	.11μ
85	120μ	.06μ
Q-8	50μ	.09μ
Q-9	50μ	.20μ

Table 2

The width information found in Table 2 was read directly by means of a traveling microscope. The thickness information was calculated from the measured resistance of the specimen and the width information tabulated above. Specimen No. Q-9 was taken as a standard and assigned a

thickness of 0.20 microns[1].

9. Conclusions.

From the data obtained through this project, one may conclude that the critical current, that is, the amount of conduction current necessary to cause a switch from the superconducting to the resistive state, is highly dependent on specimen orientation when subjected to an externally applied magnetic field. The manner in which such a magnetic field effects the critical current is, as was shown in the previous pages, a highly speculative thing. It is however possible to show, as we have done, that one might expect different effects in different orientations due to the altered patterns of anticipated current and magnetic field densities. It is not, however, a simple matter to explain the exact mode in which the interaction occurs.

For the orientation as shown in Fig. 19a, the orientation in which the greatest magnetic field effects are observed, it has been shown that the anticipated demagnetization current should be greater than than obtained in the other two orientations. This might be taken as an indication that the demagnetization current may be the responsible agent involved in the observed lowering of the critical conduction current values. Another possible avenue

---

[1] It has been optically determined that an original weight of indium of 20 mg will provide a thickness of approximately 1000 Å.

of approach to the behavior of the critical current may lie with the asymmetrical current and field density patterns which one might anticipate in this orientation. Recall it was shown in Sec. 6 that one might expect the greatest degree of asymmetry in the applied field to be present in this orientation.

For the orientations of Figs. 19b and 19c one finds it more difficult to corrolate the experimentally observed critical current variations with the anticipated field and current density patterns. It is possible, from considerations of the hypothesized current and field behavior of Secs. 4, 5 and 6, to form a model which could explain such behavior by assuming the additive effects of the demagnetization current to be greater when acting in quadrature with the conduction current than when acting with and against the conduction current where cancellation effects might exist. Such a model would however, be highly speculative at the present state of knowledge and will, therefore, be omitted.

The manner in which the magnetic field effects the critical current for any of the previously considered orientations can be seen graphically on pages 52 through 54 where critical current is plotted as a function of the applied magnetic field for various temperatures. Although insufficient data exists to establish the exact form of these curves, it is possible to gain a better perspective

as to the relative effects for the different orientations by their use.

It will be noted that Specimen Q-9 exhibited anomalous behavior when contrasted with the other specimens. This specimen appeared to anticipate the lambda jump at temperatures well above the lambda point. This specimen was one of two utilized which had been evaporated onto quartz backing. Since the other specimen showed no such anomalous behavior, it is felt that the cause was not due to the backing material. However, from considerations of the amount of indium used in the evaporation of this specimen and from resistance measurements, its thickness was determined to be about twice that of the remainder of the samples. It is thus possible that the behavior may have been due to the increased thickness; although, the work by Wright and Bird[1] would indicate to the contrary. In any case, further investigation of this point could prove helpful.

In conclusion, this project has shown the critical values of conduction current to be highly sensitive to externally applied magnetic fields and to specimen orientation within such fields. While no definite mode of interaction was established in this work, it is felt that

---

[1] Work by Wright and Bird has indicated critical current to be independent of film thickness.

increased investigation into the behavior of thin films may ultimately produce some sort of working model from which more accurate behavior predictions may be made. It is especially useful to investigate thin films since with such specimens the penetration effects are quite marked and more readily observable. It is thus hoped that this project may provide some small link in the chain of understanding which may some day explain fully the phenomenon of superconductivity.

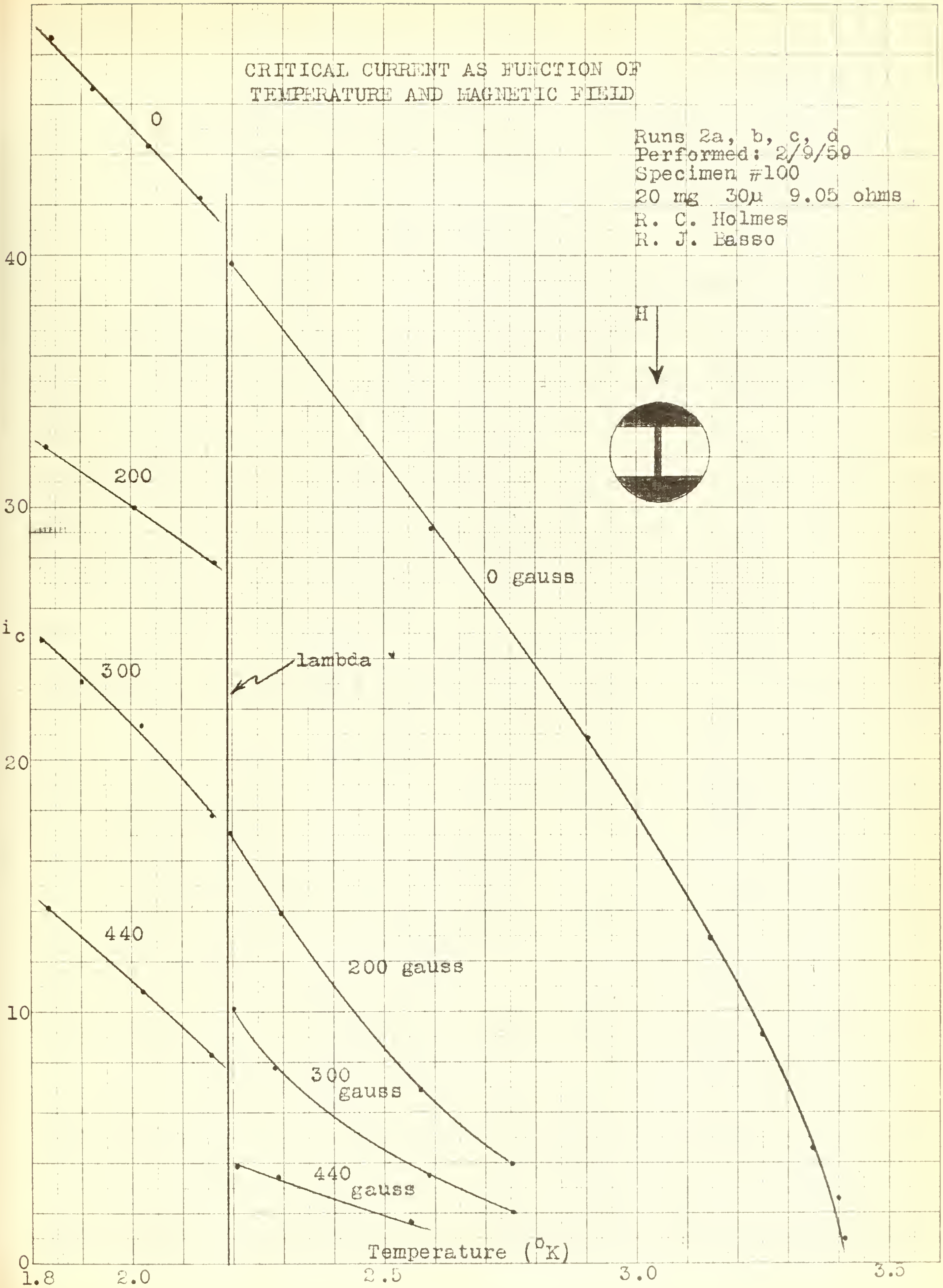

CRITICAL CURRENT AS FUNCTION OF TEMPERATURE AND MAGNETIC FIELD

Runs 2a, b, c, d
Performed: 2/9/59
Specimen #100
20 mg 30μ 9.05 ohms
R. C. Holmes
R. J. Basso

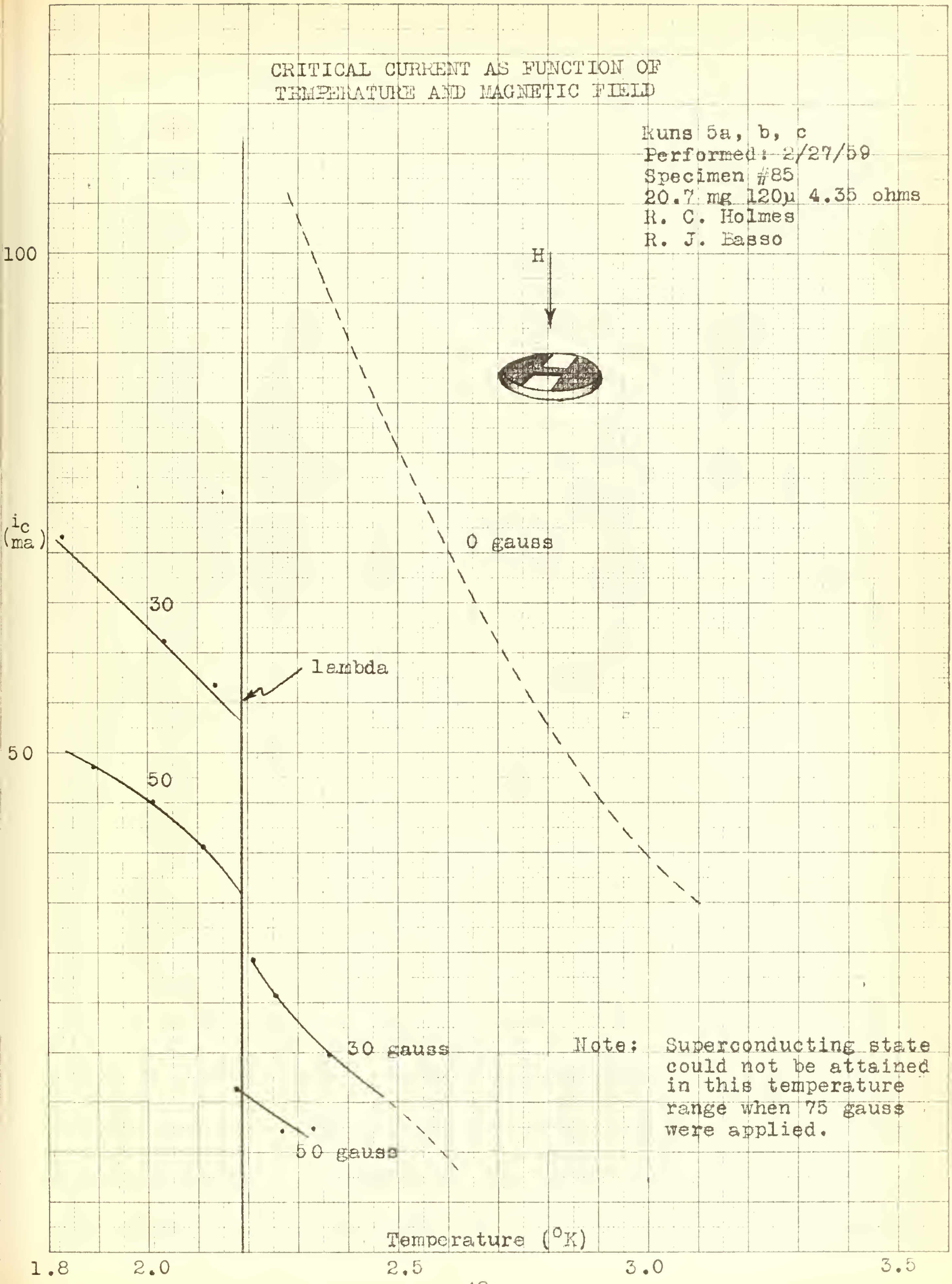

Note: Superconducting state could not be attained in this temperature range when 75 gauss were applied.

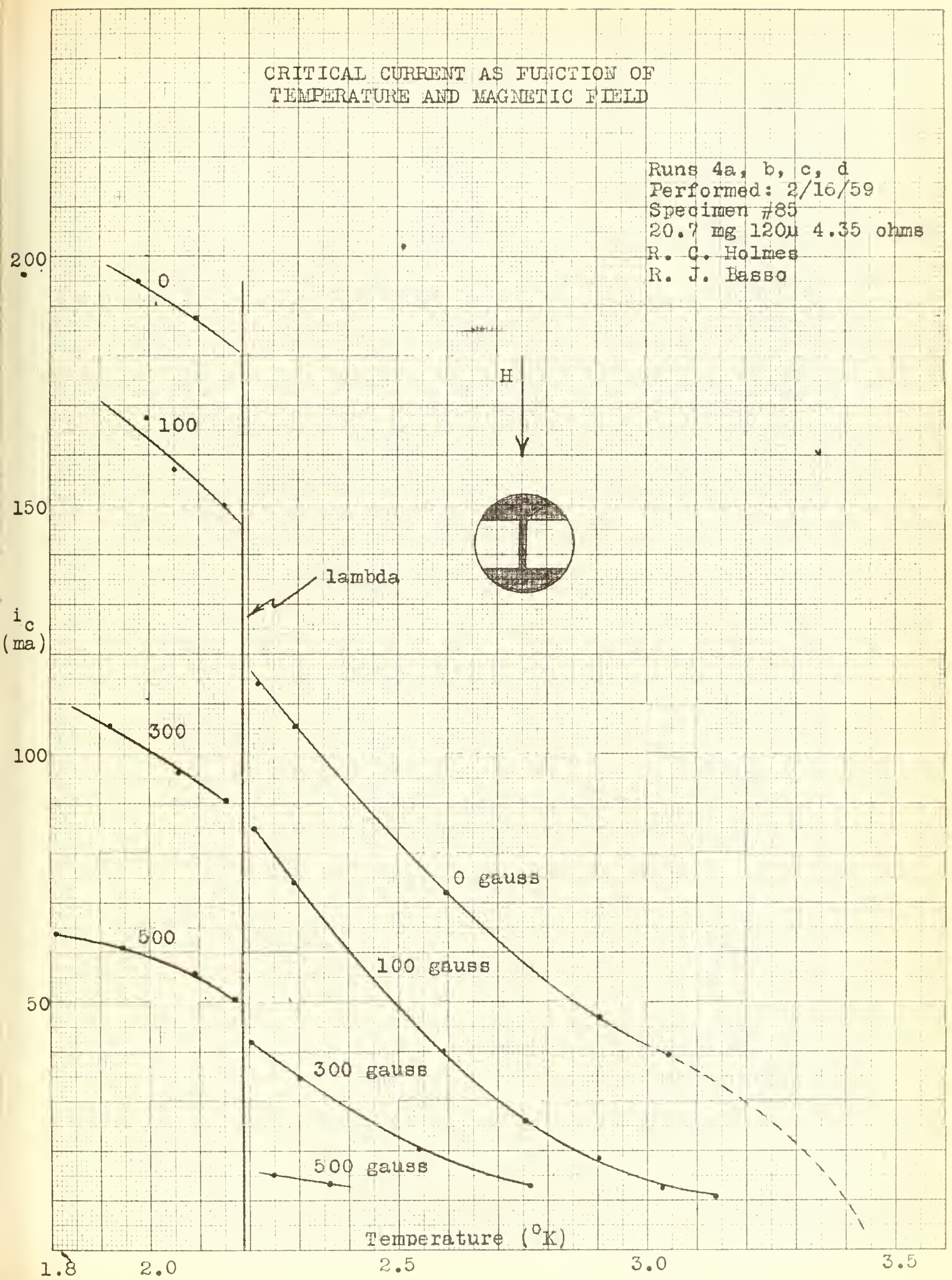

CRITICAL CURRENT AS FUNCTION OF TEMPERATURE AND MAGNETIC FIELD

Runs 4a, b, c, d
Performed: 2/16/59
Specimen #85
20.7 mg 120μ 4.35 ohms
R. C. Holmes
R. J. Basso

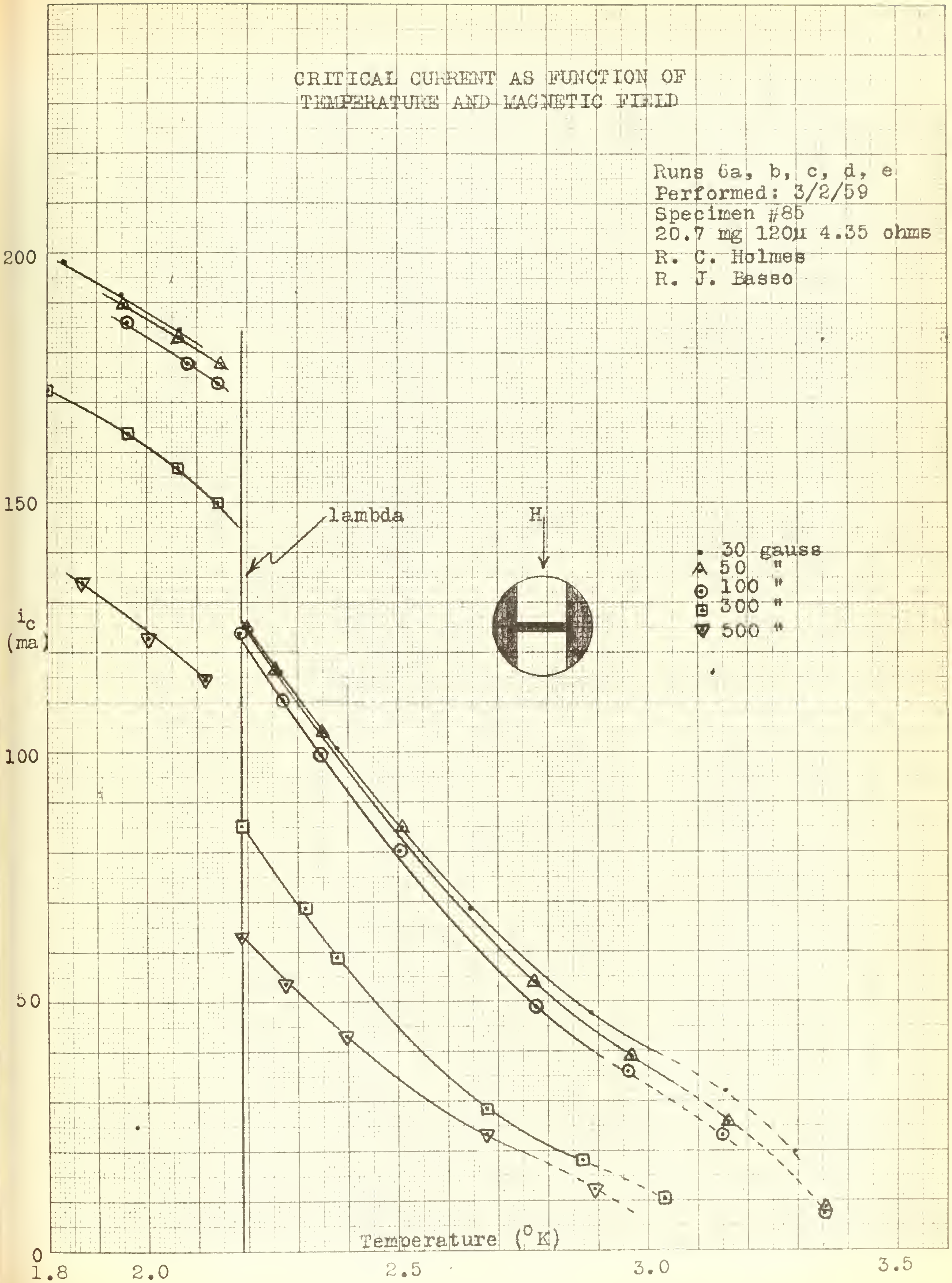

CRITICAL CURRENT AS FUNCTION OF TEMPERATURE AND MAGNETIC FIELD

Runs 6a, b, c, d, e
Performed: 3/2/59
Specimen #85
20.7 mg 120μ 4.35 ohms
R. C. Holmes
R. J. Basso

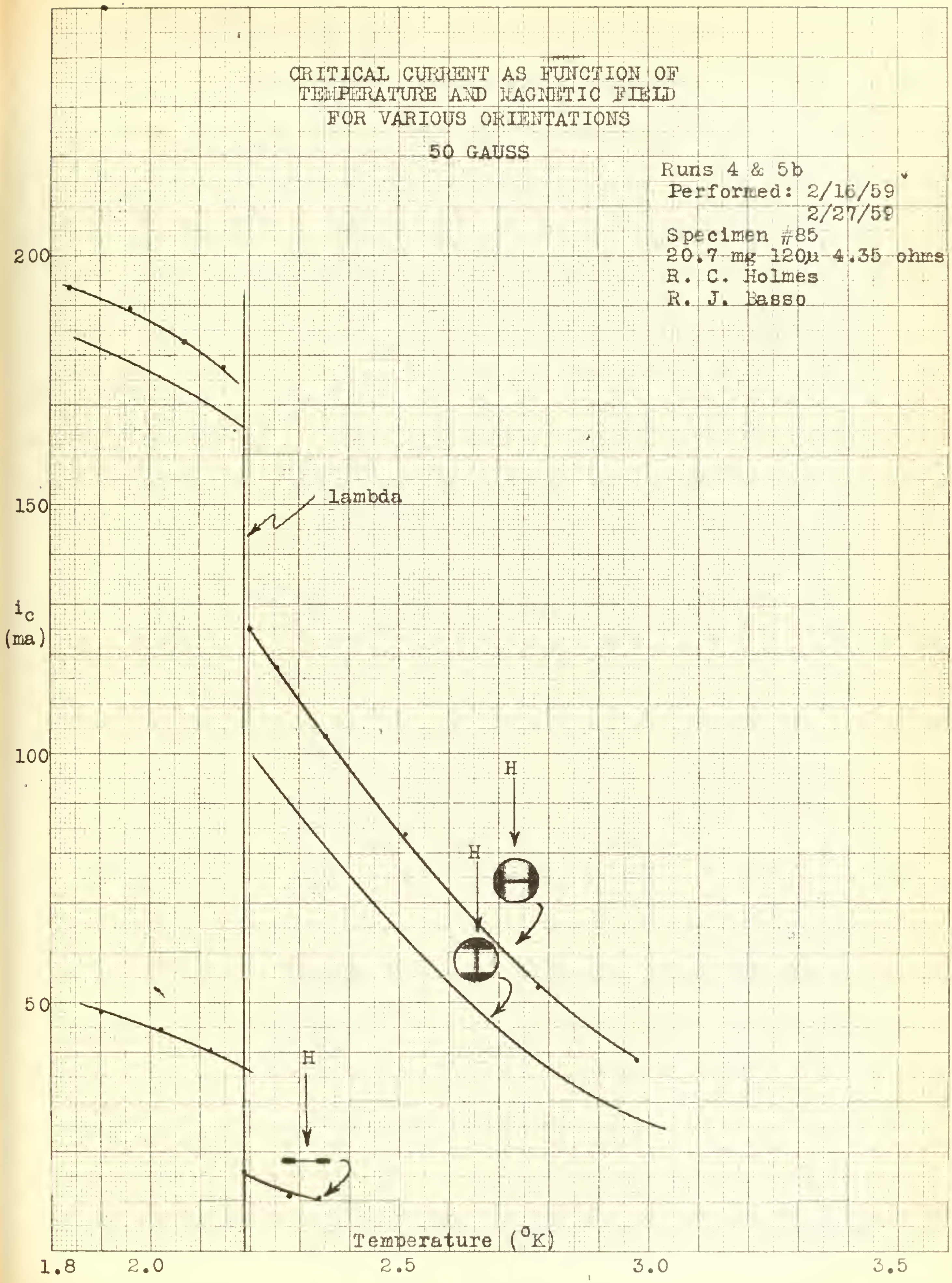

CRITICAL CURRENT AS FUNCTION OF TEMPERATURE AND MAGNETIC FIELD FOR VARIOUS ORIENTATIONS

50 GAUSS

Runs 4 & 5b
Performed: 2/16/59
2/27/59
Specimen #85
20.7 mg 120μ 4.35 ohms
R. C. Holmes
R. J. Basso

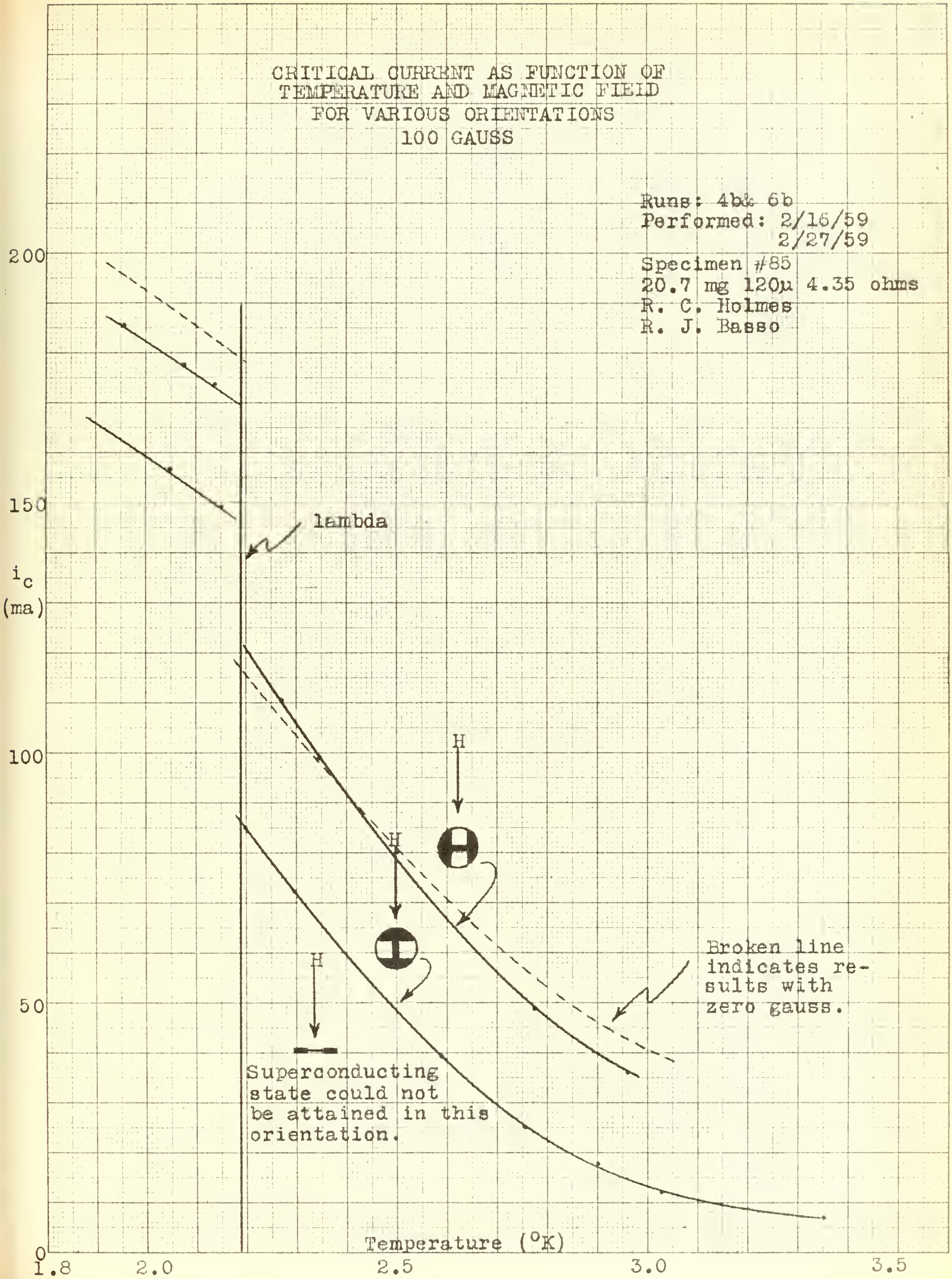

CRITICAL CURRENT AS FUNCTION OF
TEMPERATURE AND MAGNETIC FIELD
FOR VARIOUS ORIENTATIONS
100 GAUSS

Runs: 4b& 6b
Performed: 2/16/59
2/27/59
Specimen #85
20.7 mg 120µ 4.35 ohms
R. C. Holmes
R. J. Basso

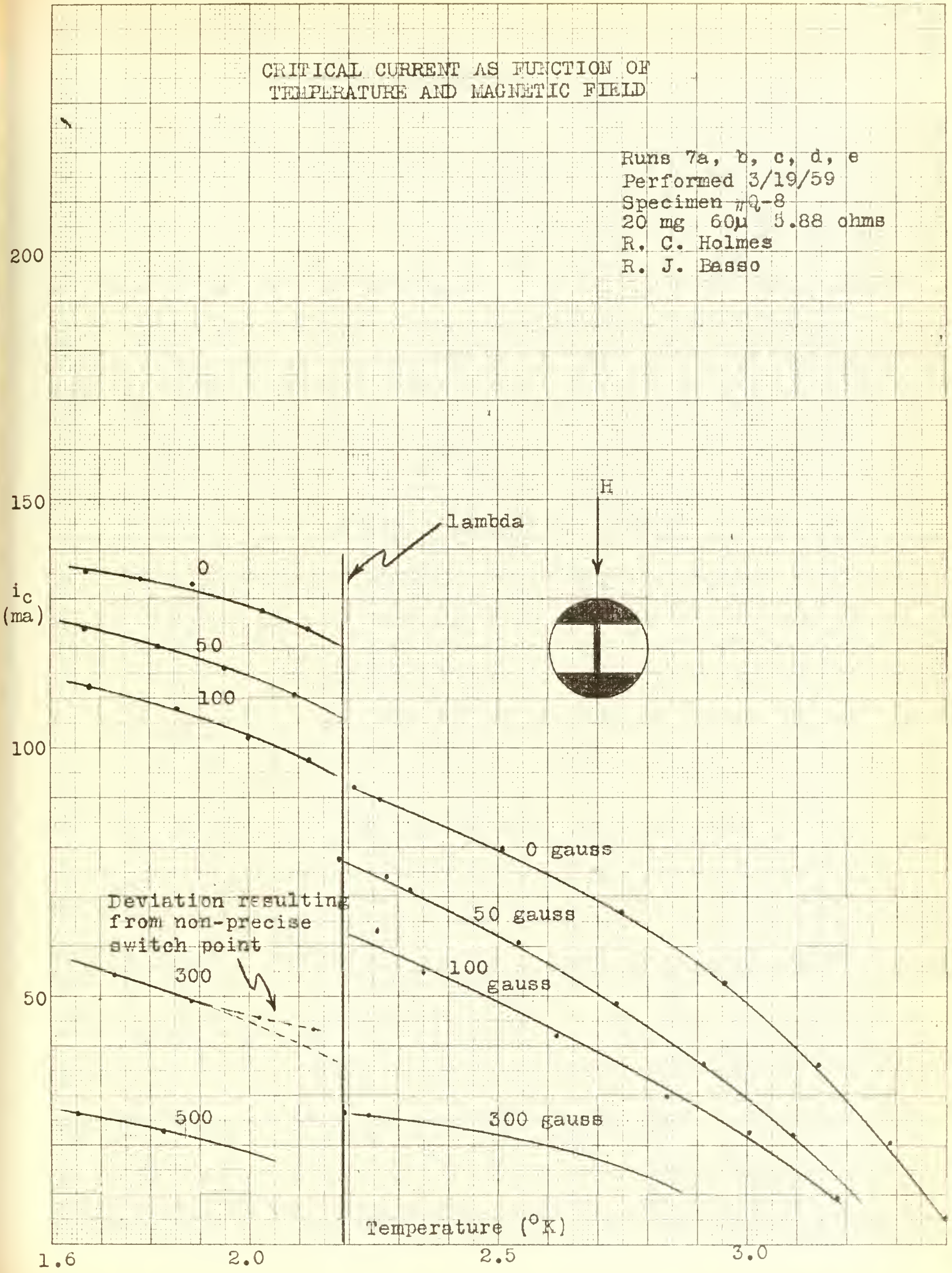

CRITICAL CURRENT AS FUNCTION OF TEMPERATURE AND MAGNETIC FIELD

Runs 7a, b, c, d, e
Performed 3/19/59
Specimen #Q-8
20 mg 60µ 5.88 ohms
R. C. Holmes
R. J. Basso

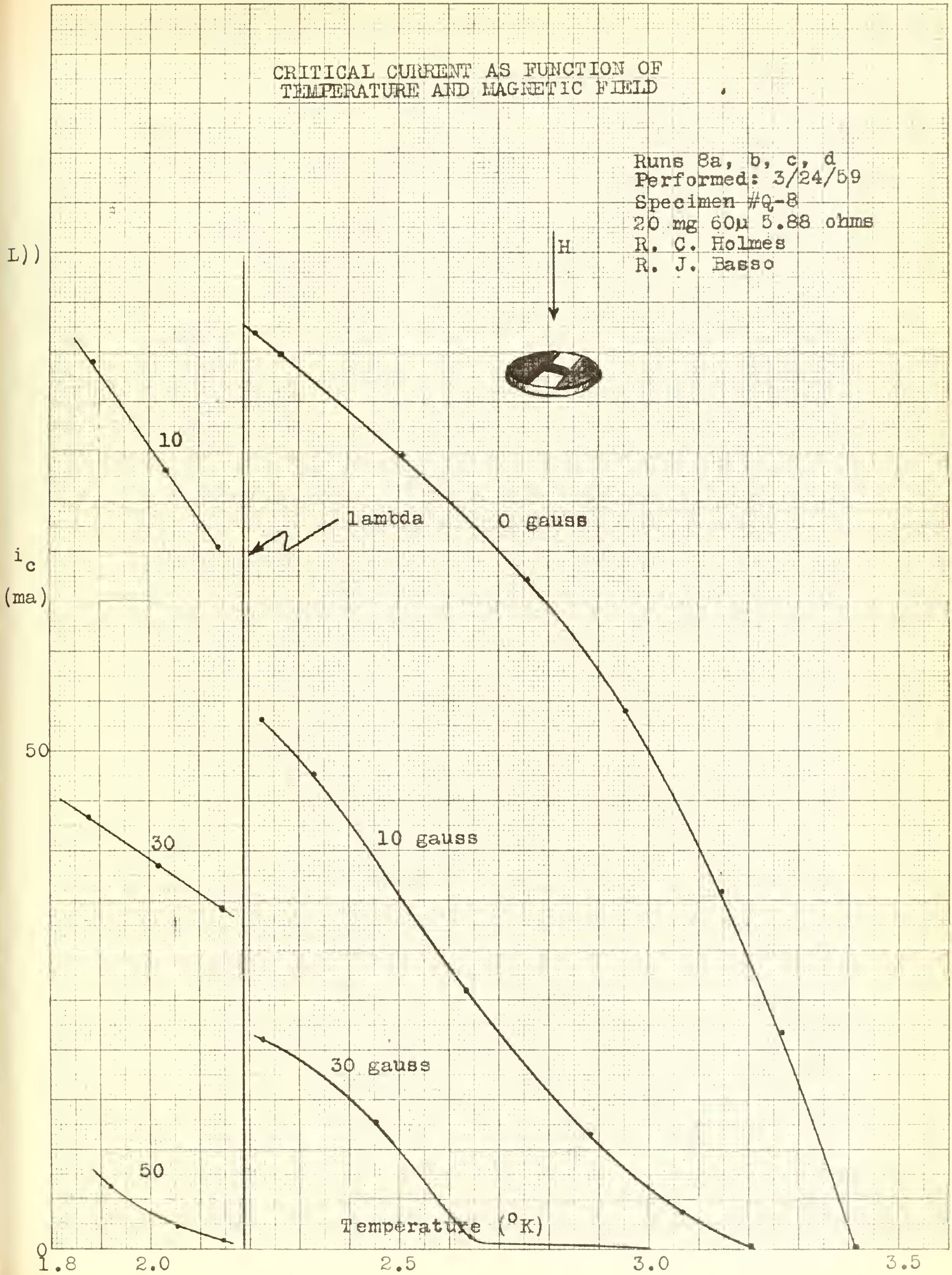

CRITICAL CURRENT AS FUNCTION OF TEMPERATURE AND MAGNETIC FIELD

Runs 8a, b, c, d
Performed: 3/24/59
Specimen #Q-8
20 mg 60µ 5.88 ohms
R. C. Holmes
R. J. Basso

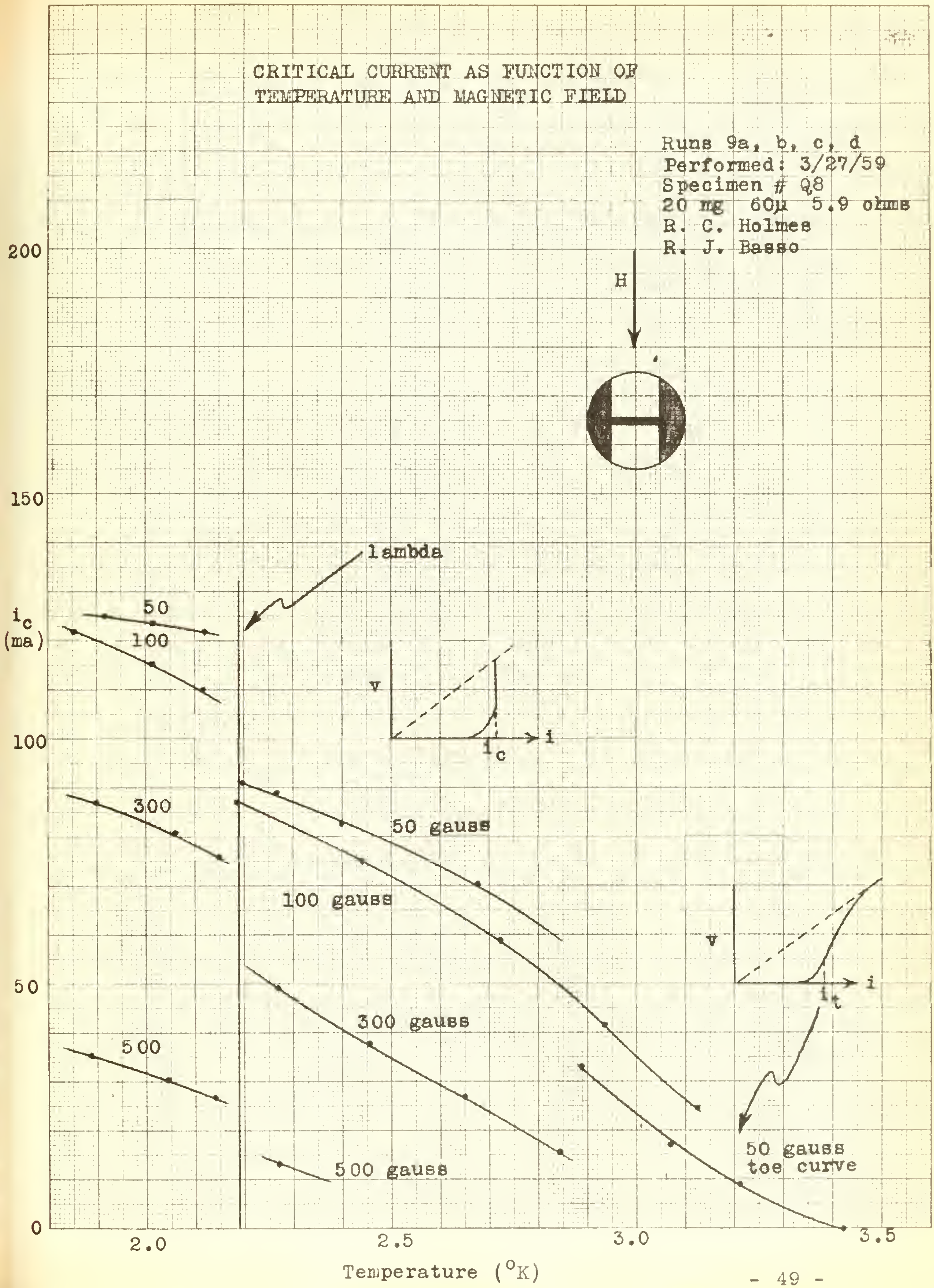

CRITICAL CURRENT AS FUNCTION OF TEMPERATURE AND MAGNETIC FIELD

Runs 9a, b, c, d
Performed: 3/27/59
Specimen # Q8
20 mg 60μ 5.9 ohms
R. C. Holmes
R. J. Basso

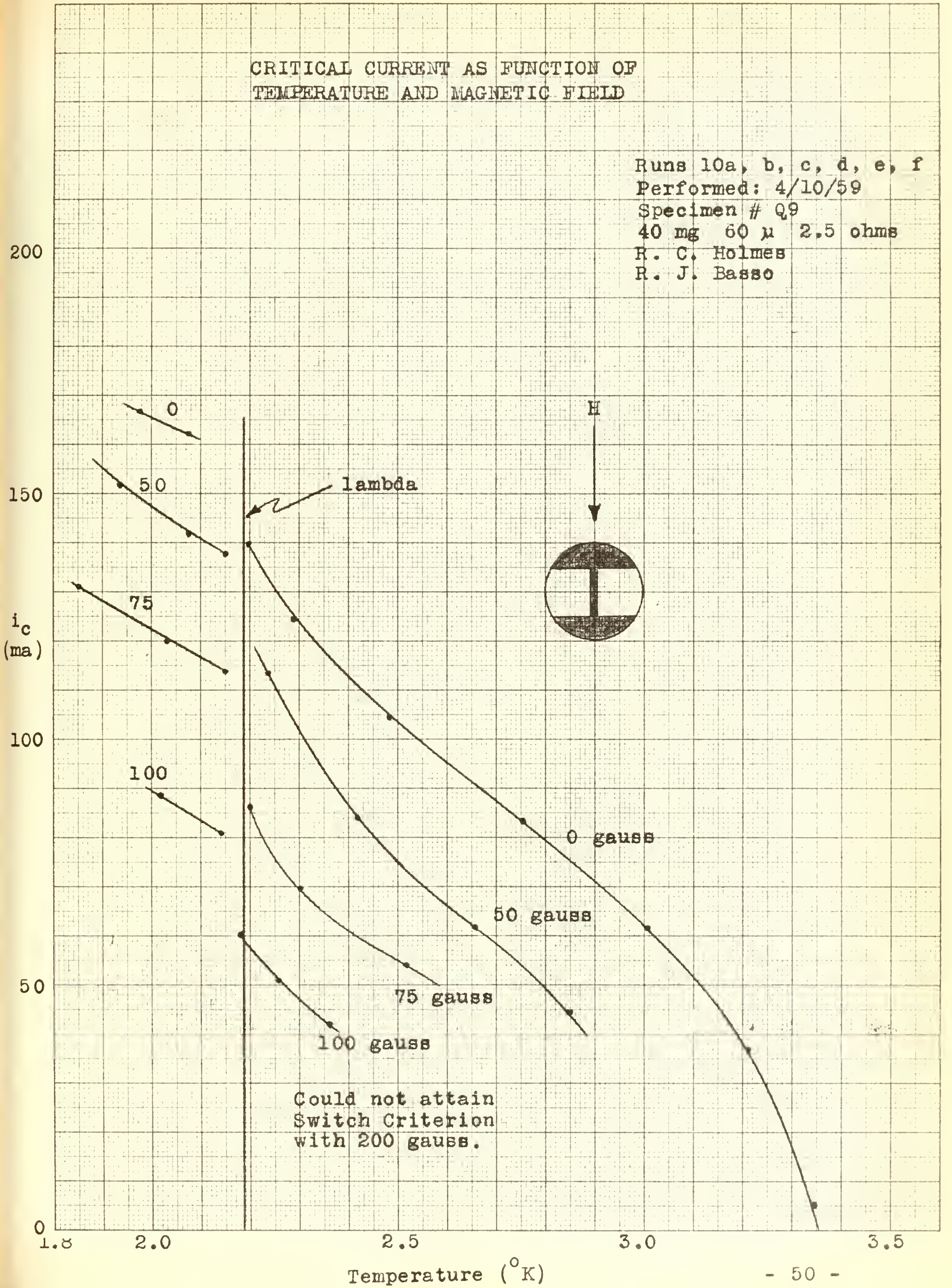
CRITICAL CURRENT AS FUNCTION OF TEMPERATURE AND MAGNETIC FIELD
Runs 10a, b, c, d, e, f
Performed: 4/10/59
Specimen # Q9
40 mg 60 μ 2.5 ohms
R. C. Holmes
R. J. Basso
H
lambda
0
50
75
100
0 gauss
50 gauss
75 gauss
100 gauss
Could not attain Switch Criterion with 200 gauss.
i_c (ma)
200
150
100
50
0
1.8
2.0
2.5
3.0
3.5
Temperature (°K)

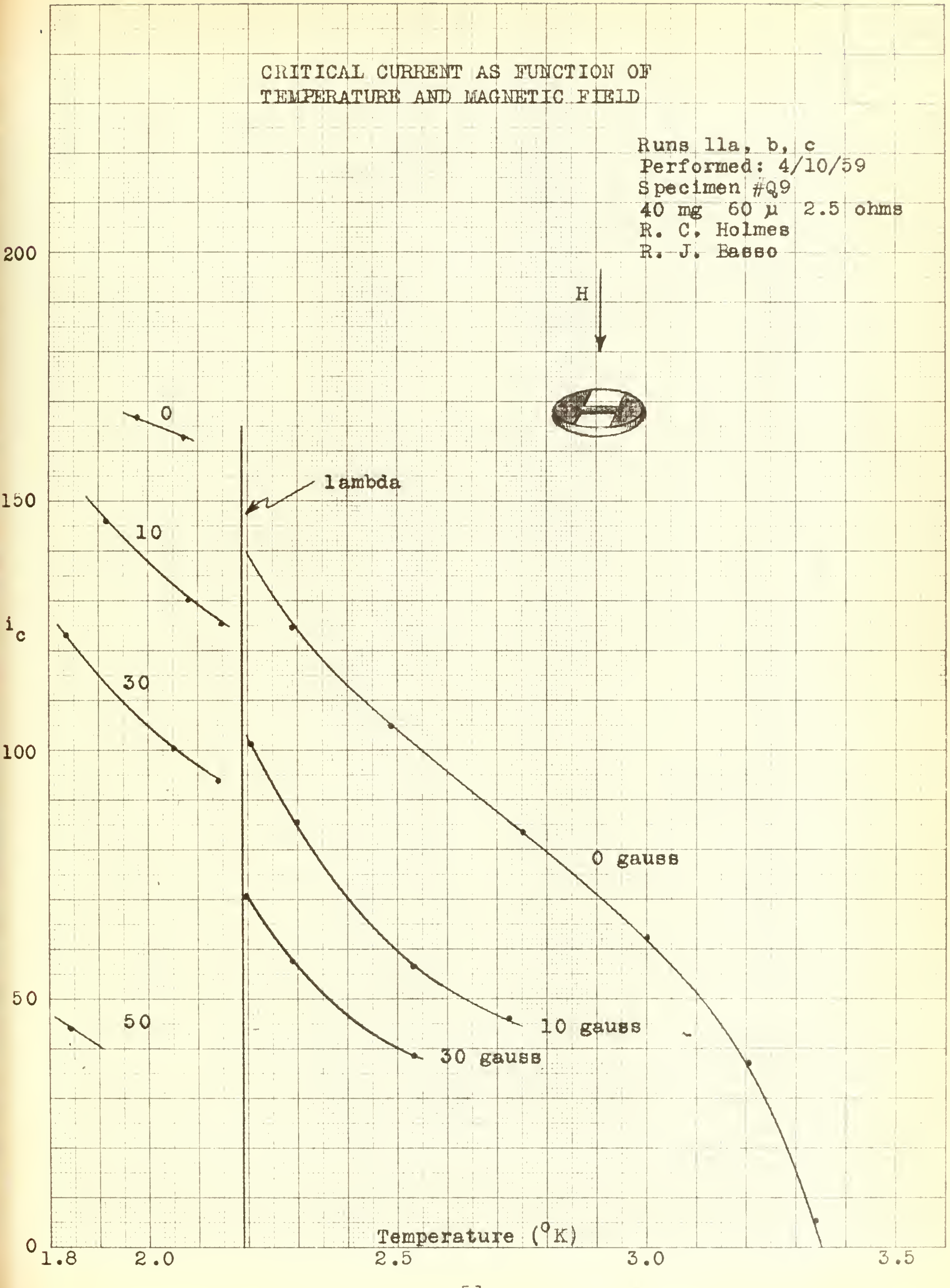

CRITICAL CURRENT AS FUNCTION OF
TEMPERATURE AND MAGNETIC FIELD

Runs 11a, b, c
Performed: 4/10/59
Specimen #Q9
40 mg 60 µ 2.5 ohms
R. C. Holmes
R. J. Basso

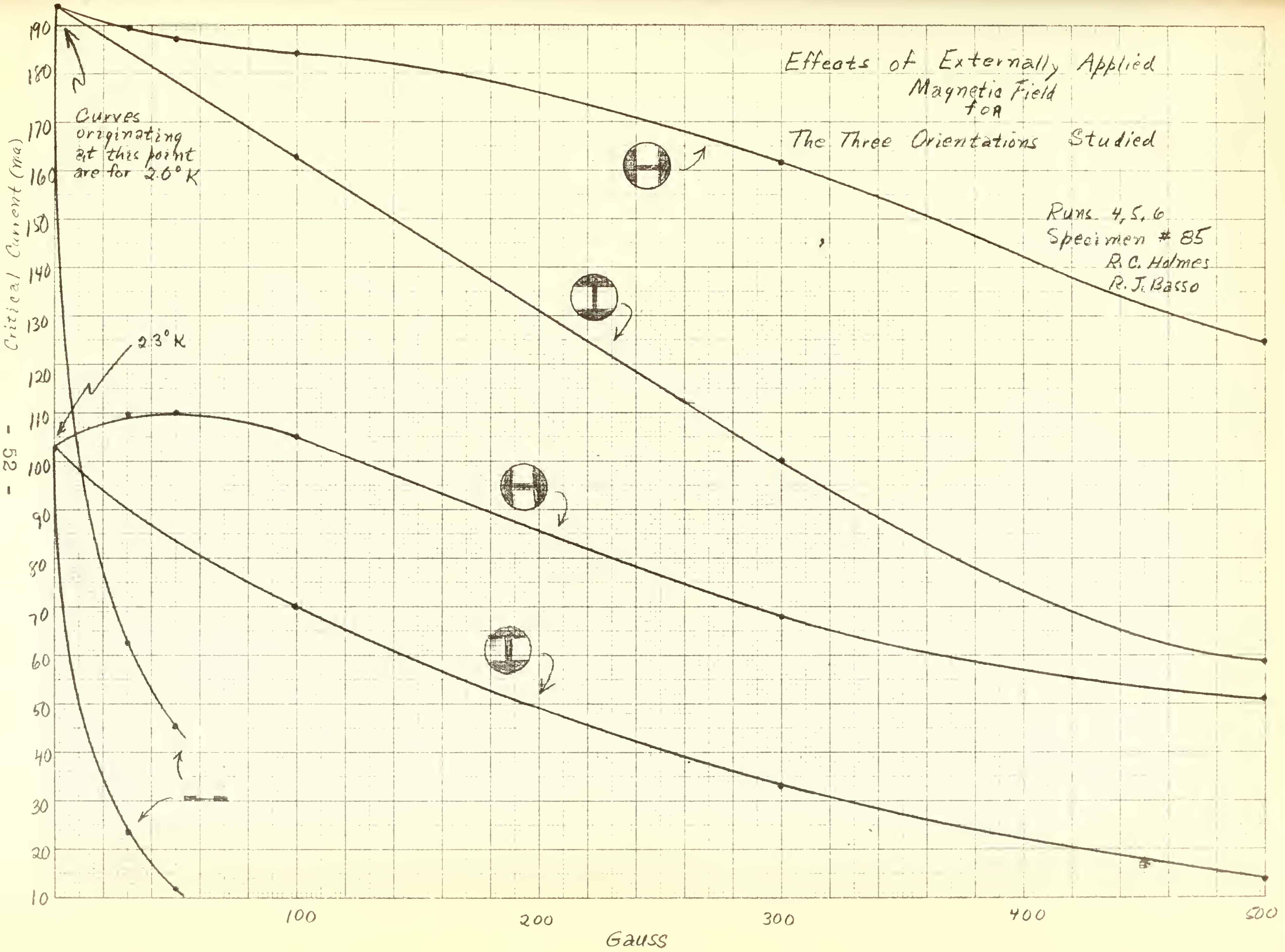
Effects of Externally Applied
Magnetic Field
for
The Three Orientations Studied
Runs 4, 5, 6
Specimen # 85
R. C. Holmes
R. J. Basso
Curves originating at this point are for 2.0° K
2.3° K
Critical Current (ma)
190
180
170
160
150
140
130
120
110
100
90
80
70
60
50
40
30
20
10
100
200
300
400
500
Gauss

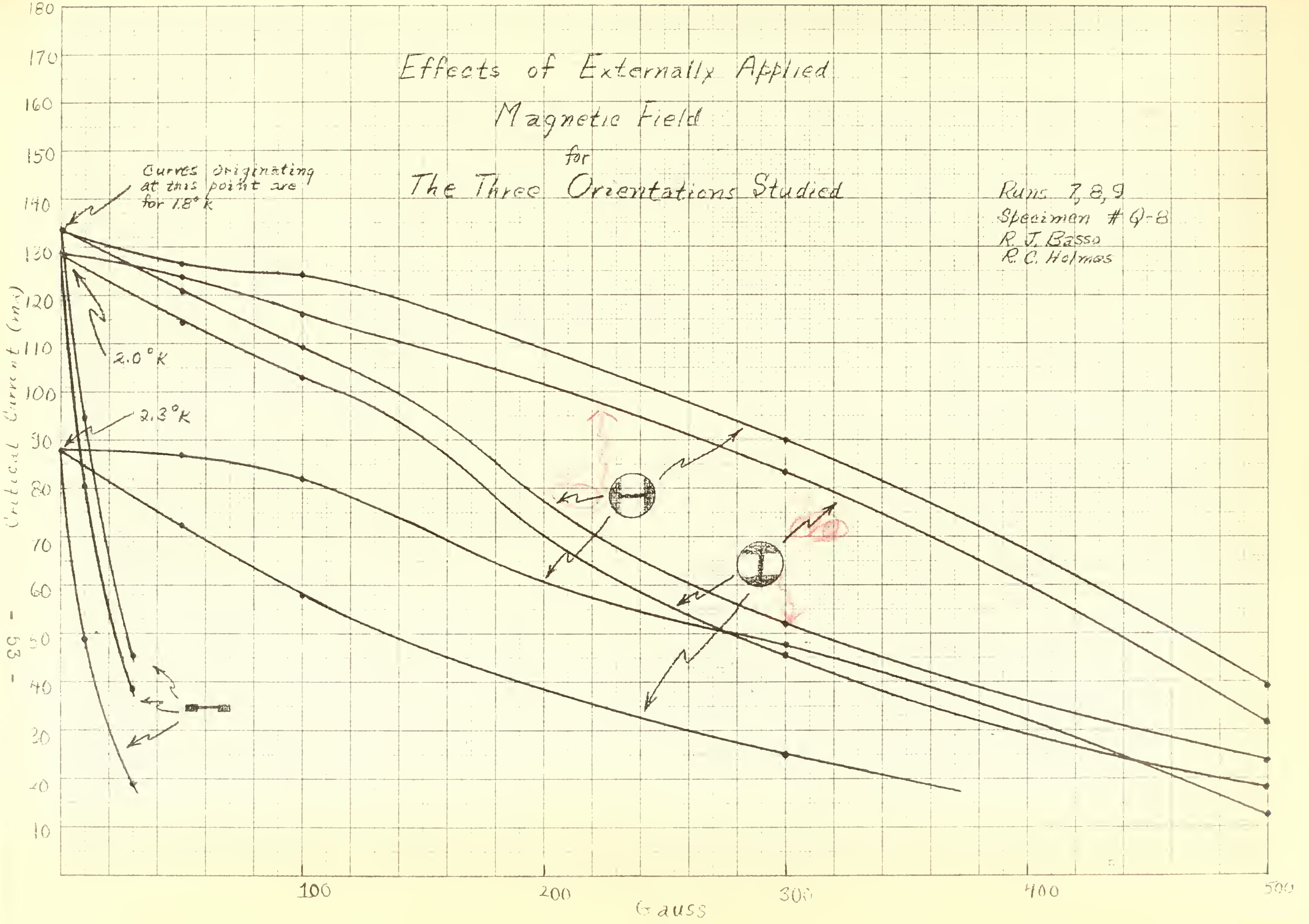

Effects of Externally Applied Magnetic Field for The Three Orientations Studied

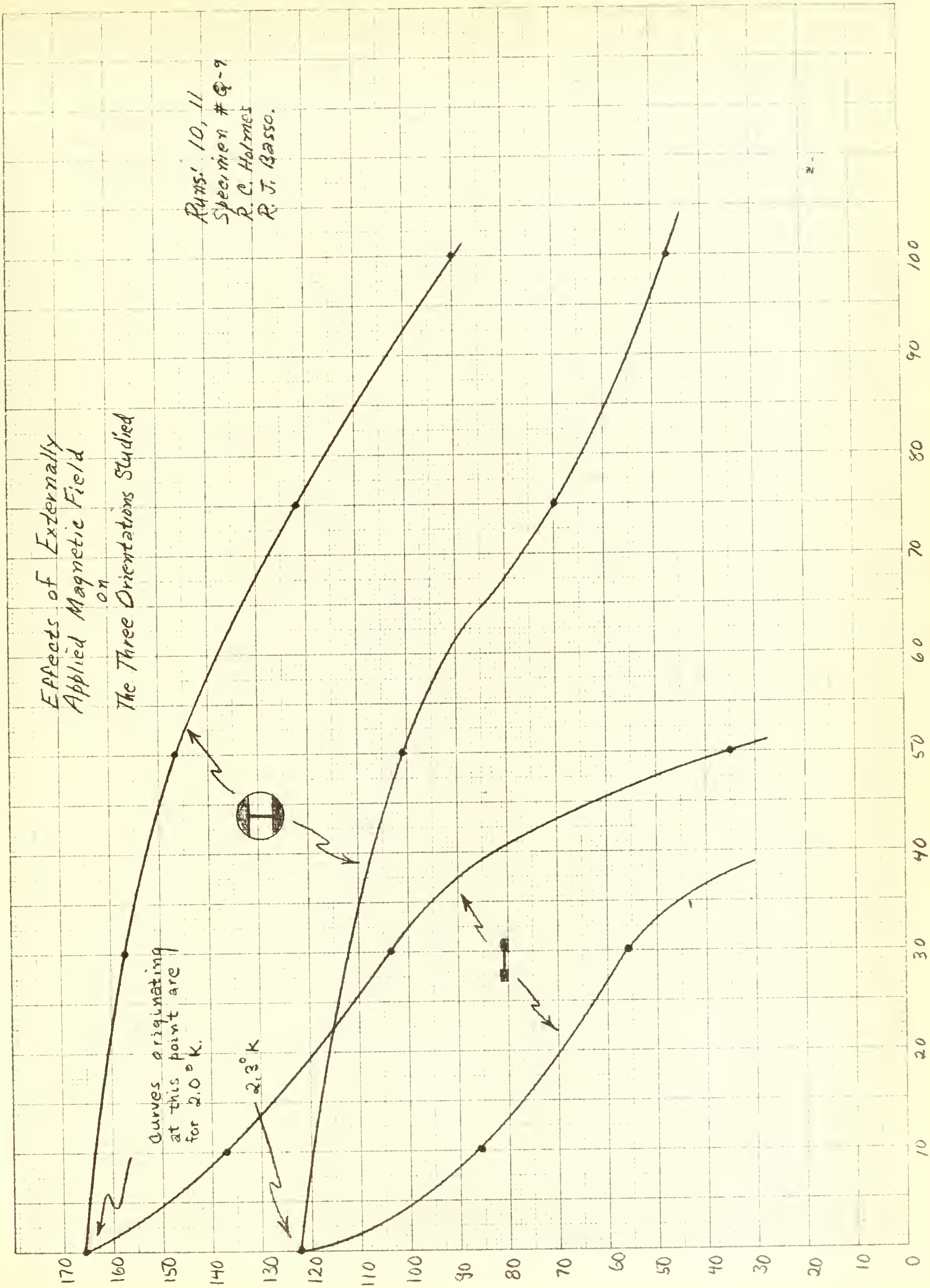
Effects of Externally
Applied Magnetic Field
on
The Three Orientations Studied
Runs: 10, 11
Specimen # Q-9
R. C. Holmes
R. J. Basso.
Curves originating at this point are for 2.0° K.
2.3° K
Gauss
0
10
20
30
40
50
60
70
80
90
100
170
160
150
140
130
120
110
100
90
80
70
60
50
40
30
20
10
0

BIBLIOGRAPHY

1. D. Schoenberg, Superconductivity, Cambridge University Press, 1952.
2. C. F. Squire, Low Temperature Physics, McGraw Hill Book Co. Inc., 1953.
3. F. E. Simon, N. Kurti, J. F. Allen and K. Mendelssohn, Low Temperature Physics, Academic Press Inc., 1952.

APPENDIX I

Proof of the Cooper solution to the London Equation

It is desired to show that the Cooper equation,

$$\overline{H} = C e^{-\frac{a+b}{\sqrt{2}\lambda}} \left[\hat{\imath}\ (e^{\frac{x}{\sqrt{2}\lambda}} + e^{-\frac{x}{\sqrt{2}\lambda}})(e^{-\frac{y}{\sqrt{2}\lambda}} - e^{\frac{y}{\sqrt{2}\lambda}}) + \hat{\jmath}\ (e^{\frac{x}{\sqrt{2}\lambda}} - e^{-\frac{x}{\sqrt{2}\lambda}})(e^{\frac{y}{\sqrt{2}\lambda}} + e^{-\frac{y}{\sqrt{2}\lambda}})\right],$$

is a solution to the London equation,

$$\nabla^2 \overline{H} = \frac{\overline{H}}{\lambda^2}$$

One may proceed in the following manner; let

$$C_1 = C e^{-\frac{a+b}{\sqrt{2}\lambda}}$$

$$X = (e^{\frac{x}{\sqrt{2}\lambda}} + e^{-\frac{x}{\sqrt{2}\lambda}})$$

$$X' = (e^{\frac{x}{\sqrt{2}\lambda}} - e^{-\frac{x}{\sqrt{2}\lambda}})$$

$$Y = (e^{\frac{y}{\sqrt{2}\lambda}} + e^{-\frac{y}{\sqrt{2}\lambda}})$$

$$Y' = (e^{-\frac{y}{\sqrt{2}\lambda}} - e^{\frac{y}{\sqrt{2}\lambda}})$$

then

$$\frac{\partial X}{\partial x} = \frac{1}{\sqrt{2}\lambda}(e^{\frac{x}{\sqrt{2}\lambda}} - e^{-\frac{x}{\sqrt{2}\lambda}})$$

$$\frac{\partial X'}{\partial x} = \frac{1}{\sqrt{2}\lambda}(e^{\frac{y}{\sqrt{2}\lambda}} + e^{-\frac{x}{\sqrt{2}\lambda}})$$

$$\frac{\partial Y}{\partial y} = \frac{1}{\sqrt{2}\lambda}(e^{\frac{y}{\sqrt{2}\lambda}} - e^{-\frac{y}{\sqrt{2}\lambda}})$$

$$\frac{\partial Y'}{\partial y} = \frac{1}{\sqrt{2}\lambda}(e^{\frac{y}{\sqrt{2}\lambda}} + e^{-\frac{y}{\sqrt{2}\lambda}})$$

also

$$\frac{\partial^2 X}{\partial x^2} = \frac{X}{2\lambda^2} \qquad \frac{\partial^2 X'}{\partial x^2} = \frac{X'}{2\lambda^2}$$

$$\frac{\partial^2 Y}{\partial y^2} = \frac{Y}{2\lambda^2} \qquad \frac{\partial^2 Y'}{\partial y^2} = \frac{Y'}{2\lambda^2} .$$

Thus, making the appropriate substitutions, the Cooper equation becomes

$$\overline{H} = C_1\left[\hat{\imath}\ XY' + \hat{\jmath}\ X'Y\right] \qquad \text{(I-1)}$$

Now, if one calls $A = XY'$ and $A' = X'Y$, the Cooper equation may be written as

$$\bar{H} = C_1 \left(A\,\hat{i} + A'\,\hat{j} \right) \quad . \qquad \text{(I-2)}$$

From Eq. (I-1) one finds

$$\nabla^2 \bar{H} = C_1 \left[\hat{i}\,\frac{\partial^2 X}{\partial x^2} Y' + \hat{j}\,\frac{\partial^2 X'}{\partial x^2} Y + \hat{i}\,\frac{\partial^2 Y'}{\partial y^2} X + \hat{j}\,\frac{\partial^2 Y}{\partial y^2} X' \right].$$

Substitution of the appropriate symbols for the above second partials we have,

$$\nabla^2 \bar{H} = \frac{C_1}{\lambda^2} \left(X\,Y'\,\hat{i} + X'\,Y\,\hat{j} \right) \quad ,$$

which can also be written

$$\nabla^2 \bar{H} = \frac{C_1}{\lambda^2} \left(A\,\hat{i} + A'\,\hat{j} \right) . \qquad \text{(I-3)}$$

But, from equation (I-2) one can see that Eq. (I-3) is no more than

$$\nabla^2 \bar{H} = \frac{H}{\lambda^2} \quad . \qquad \text{Q.E.D.}$$

APPENDIX II

Table of Data

Run #2, Specimen #100, Width 30 μ, Resistance 9.1 ohms
Evaporation of 20 mg of Indium

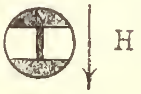

Run # 2a (Zero gauss)

Pressure* (oil)(mm)	Pressure (Hg)(mm)	Temperature °K	DC current (ma)
	293.0	3.349	4.5
	257.0	3.250	9.1
	195.0	3.050	16.0
	122.5	2.752	25.0
	92.0	2.593	29.1
735	48.8	2.288	32.5
591	39.3	2.196	39.8
547	36.4	2.165	42.0
389	25.8	2.034	44.4
281	18.7	1.925	46.7
214	14.3	1.843	48.8

Run # 2b (200 gauss)

Pressure* (oil)(mm)	Pressure (Hg)(mm)	Temperature °K	DC current (ma)
	87.0	2.569	6.8
747	49.7	2.296	13.8
590	39.2	2.195	17.1
524	34.8	2.147	27.6
359	23.9	2.007	30.0
207	13.8	1.832	32.4
134	8.92	1.713	35.9

Run # 2c (300 gauss)

Pressure* (oil) (mm)	Pressure (Hg) (mm)	Temperature (^oK)	DC current (ma)
730	48.5	2.284	7.7
598	39.8	2.201	10.1
536	36.0	2.160	17.7
373	24.8	2.020	21.3
266	17.7	1.908	23.0
203	13.5	1.826	24.8

Run # 2d (400 gauss)

612	40.6	2.209	3.8
542	36.0	2.160	8.2
380	25.25	2.026	10.7
210	13.9	1.834	14.1

Run # 2e (200 gauss)

	122.0	2.750	6.0
	90.5	2.610	9.4
739	49.1	2.290	18.0
592	39.3	2.196	21.4
522	34.7	2.146	28.2
391	26.0	2.037	30.2
296	19.7	1.942	32.1
200	13.3	1.821	34.7

* Conversion factor of 15.05 applies.

Run #4, Specimen # 85, Width 120 µ, Resistance 4.3 ohms

Evaporation of 20.7 mg of Indium

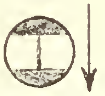

Run # 4a (Zero gauss)

Pressure* (oil) (mm)	Pressure (Hg) (mm)	Temperature $(^{\circ}K)$	DC current (ma)
	319.8	3.419	5.5
	251.8	3.234	25.3
	191.5	3.037	38.0
	155.0	2.897	45.8
	92.0	2.593	71.0
733	48.75	2.287	105.0
621	41.0	2.213	113.5
454	30.2	2.092	187.0
330	21.9	1.977	195.0

Run # 4b (100 gauss)

	223.0	3.144	9.1
	192.5	3.041	11.2
	155.0	2.897	17.3
	122.0	2.750	24.9
	90.5	2.584	39.1
736	48.9	2.288	72.0
588	39.1	2.194	85.2
527	35.0	2.149	149.5
403	26.8	2.048	157.0
229	15.2	1.860	167.0

Run # 4c (300 gauss)

Pressure* (oil) (mm)	Pressure (Hg) (mm)	Temperature (°K)	DC current (ma)
	123.0	2.755	11.6
	82.0	2.533	19.1
	50.0	2.298	33.8
590	39.2	2.195	41.0
525	34.9	2.148	90.0
413	27.5	2.057	95.5
272	18.1	1.915	105.2

Run # 4d (500 gauss)

	56.5	2.352	12.1
653	43.5	2.238	14.2
549	36.5	2.166	49.5
446	29.8	2.087	55.0
309	20.6	1.956	60.0
187	12.5	1.803	63.0

* Conversion factor of 15.05 applies

Run #5, Specimen # 85, Width 120 μ, Resistance 4.3 ohms
Evaporation of 20.7 mg of Indium

Run # 5a (30 gauss)

Pressure** (oil) (mm)	Pressure (Hg) (mm)	Temperature (°K)	DC current (ma)
	94.0	2.604	9.4
	58.0	2.364	19.6
623	45.8	2.260	25.5
559	41.1	2.214	29.2
462	33.9	2.137	56.5
348	25.6	2.031	61.0
187	13.7	1.830	71.5

Run # 5b (50 gauss)

640	47.1	2.272	11.2
519	38.2	2.184	16.2
432	31.7	2.111	40.7
330	24.3	2.011	45.0
232	17.0	1.895	48.5

Run # 5c (75 gauss)

Unable to attain the superconducting state

Run # 5d (10 gauss)

	261.0	3.261	11.6
	201.0	3.072	20.4
	153.0	2.889	32.4
	96.0	2.616	62.4
260	19.1	1.932	189.0

Run #6, Specimen # 85, Width 120 μ, Resistance 4.3 ohms
Evaporation of 20.7 mg of Indium

Run # 6a (30 gauss)

Pressure** (oil) (mm)	Pressure (Hg) (mm)	Temperature (°K)	DC current (ma)
	270.5	3.288	19.1
	225.0	3.151	31.6
	152.5	2.887	46.9
	101.0	2.644	68.5
	59.0	2.372	100.8
614	45.2	2.225	116.4
543	40.0	2.203	124.3
469	34.5	2.144	178.0
373	27.4	2.856	185.0
275	20.2	1.950	192.0
190	13.9	1.835	199.0

Run # 6b (50 gauss)

Pressure** (oil) (mm)	Pressure (Hg) (mm)	Temperature (°K)	DC current (ma)
	293.5	3.350	7.3
	227.0	3.157	25.0
	172.0	2.965	38.8
	126.0	2.770	53.7
	78.0	2.507	83.9
766	56.0	2.348	103.7
611	44.8	2.251	116.8
532	39.1	2.194	125.2
471	34.7	2.146	178.0
380	27.9	2.062	183.0

Run # 6b (cont.)

Pressure** (oil) (mm)	Pressure (Hg) (mm)	Temperature (°K)	DC current (ma)
279	20.6	1.956	190.0
186	13.7	1.830	194.0

Run # 6c (100 gauss)

	293.5	3.350	6.3
	223.0	3.144	22.7
	170.0	2.958	35.4
	126.5	2.772	48.5
	77.0	2.501	80.0
754	55.4	2.342	98.9
637	46.7	2.268	110.0
517	38.0	2.182	124.0
467	34.3	2.141	174.0
398	29.3	2.081	178.0
267	19.6	1.960	186.0

Run # 6d (300 gauss)

	190.0	3.032	9.8
	147.5	2.865	17.6
	106.0	2.671	27.8
	59.5	2.376	58.3
696	51.2	2.310	68.8
523	38.4	2.186	85.3
465	34.2	2.140	150.0
378	27.8	2.061	157.0
285	20.9	1.961	164.0
169	12.4	1.801	173.0

Run # 6e (500 gauss)

Pressure** (oil) (mm)	Pressure (Hg) (mm)	Temperature (°K)	DC current (ma)
	152.5	2.888	11.7
	106.0	2.671	23.0
	62.0	2.395	42.7
645	47.5	2.275	53.0
524	38.5	2.187	62.8
441	32.4	2.119	114.6
321	23.7	2.004	123.0
214	15.7	1.871	134.0

** Conversion factor of 13.6 applies

Run #7, Specimen # Q-8, Width 60 μ, Resistance 7.0 ohms
Evaporation of 20 mg of Indium

Run # 7a (Zero gauss)

Pressure** (oil) (mm)	Pressure (Hg) (mm)	Temperature (°K)	DC current (ma)
	313.0	3.402	5.2
	269.0	3.284	20.5
	223.5	3.145	36.3
	169.0	2.954	53.0
	121.5	2.748	67.2
	77.5	2.504	79.8
618	45.4	2.257	89.9
544	40.0	2.203	92.0
439	32.2	2.118	123.9
341	25.0	2.023	127.8
223	16.4	1.884	133.1
156	11.5	1.779	134.2
102	7.5	1.668	135.8

Run # 7b (50 gauss)

	207.5	3.092	22.1
	158.0	2.910	36.5
	118.5	2.733	48.6
	82.5	2.536	60.8
	52.5	2.320	71.7
645	47.5	2.275	73.7
522	37.7	2.179	77.8

Run # 7b (cont.)

Pressure** (oil) (mm)	Pressure (Hg) (mm)	Temperature (°K)	DC current (ma)
405	29.8	2.087	110.8
273	20.1	1.948	116.1
177	13.0	1.815	120.2
101	7.4	1.665	124.1
67	4.9	1.569	126.2
	Run # 7c (100 gauss)		
	235.0	3.183	9.2
	181.5	3.001	22.7
	140.0	2.833	29.9
	95.5	2.613	42.0
	56.0	2.348	55.0
614	45.2	2.254	63.1
439	32.2	2.117	97.5
317	23.3	1.998	102.0
202	14.8	1.853	108.0
108	7.81	1.679	112.2
	Run # 7d (300 gauss)		
591	43.5	2.238	25.8
524	38.6	2.188	26.5
449	33.1	2.127	43.4
337	24.8	2.020	45.9
223	16.4	1.884	49.0
128	9.4	1.726	54.1

Run # 7e (500 gauss)

Pressure** (oil) (mm)	Pressure (Hg) (mm)	Temperature (^{o}K)	DC current (ma)
184	13.5	1.826	23.0
97	7.1	1.655	26.6

** Conversion factor of 13.6 applies.

Run #8, Specimen # Q-8, Width 60 µ, Resistance 7.0 ohms
Evaporation of 20 mg of Indium

Run # 8a (Zero gauss)

Data consistent with Run # 7a

Run # 8b (10 gauss)

	150.0	2.877	11.5
	99.0	2.633	25.8
	53.5	2.328	47.7
573	42.2	2.225	53.0
459	33.8	2.135	70.5
347	25.5	2.030	78.0
201	14.8	1.885	89.0

Run # 8c (30 gauss)

	70.5	2.456	12.6
570	41.9	2.223	21.0
470	34.6	2.145	34.2
336	24.7	2.018	38.4
217	16.0	1.877	43.3

Run # 8d (50 gauss)

Pressure** (oil) (mm)	Pressure (Hg)(mm)	Temperature (^{o}K)	DC current (ma)
467	34.4	2.142	0.9
372	27.3	2.054	2.2
252	18.5	1.922	6.3

** Conversion factor of 13.6 applies.

Run #9, Specimen # Q-8, Width 60 μ, Resistance 7.0 ohms
Evaporation of 20 mg of Indium

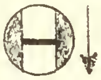

Run # 9a (50 gauss)

	245.0	3.214	9.5
	200.5	3.068	17.0
	152.5	2.888	33.5
	106.0	2.671	70.0
	62.0	2.395	83.0
626	46.0	2.262	89.0
533	39.2	2.195	91.0
437	32.2	2.117	122.0
328	24.2	2.011	123.5
244	17.9	1.912	125.0

Run # 9b (100 gauss)

	217.0	3.124	25.0
	164.0	2.934	41.5

Run # 9b (cont.)

Pressure** (oil) (mm)	Pressure (Hg) (mm)	Temperature (°K)	DC current (ma)
	116.0	2.722	59.0
	68.0	2.439	75.0
517	38.0	2.182	87.0
435	32.0	2.114	110.0
327	24.1	2.010	116.0
201	14.7	1.850	122.0
	Run # 9c (300 gauss)		
	142.0	2.842	15.7
	102.0	2.649	26.8
	70.0	2.453	37.7
552	40.7	2.271	49.5
475	35.0	2.149	76.0
373	27.4	2.056	81.0
232	17.1	1.897	87.0
	Run # 9d (500 gauss)		
658	47.4	2.275	13.5
465	34.2	2.140	27.0
363	26.7	2.046	30.5
230	16.9	1.894	35.5

** Conversion factor of 13.6 applies.

Run #10, Specimen # Q-9, Width 60 u, Resistance 2.5 ohms
Evaporation of 40 mg of Indium

Run # 10a (Zero gauss)

Pressure** (oil) (mm)	Pressure (Hg) (mm)	Temperature (^oK)	DC current (ma)
	291.0	3.344	4.8
	242.5	3.206	37.0
	181.0	2.999	62.0
	122.0	2.750	83.5
	74.0	2.481	104.5
645	48.5	2.285	124.5
515	38.9	2.192	140.2
385	28.3	2.068	163.0
293	21.5	1.971	167.0
	Run # 10b (50 gauss)		
	141.5	2.840	45.0
	102.0	2.649	61.5
	64.0	2.410	84.0
580	42.6	2.230	114.0
472	34.7	2.146	138.0
386	28.4	2.069	142.0
258	19.0	1.930	152.0

** Conversion factor of 13.6 applies.

Run # 10c (100 gauss)

Pressure** (oil) (mm)	Pressure (Hg) (mm)	Temperature (^{o}K)	DC current (ma)
	57.0	2.356	42.0
611	45.0	2.253	51.0
511	37.6	2.178	60.0
465	34.2	2.140	81.0
334	24.6	2.017	89.0

Run # 10d (300 gauss)

Unable to attain superconducting state

Run # 10e (200 gauss)

Unable to attain superconducting state

** Conversion factor of 13.6 applies

Run # 10f (75 gauss)

	79.0	2.513	54.0
	50.0	2.298	70.0
530	39.0	2.193	87.0
457	34.6	2.145	114.0
347	25.5	2.030	120.0
197	14.5	1.847	131.0

Run #11, Specimen # Q-9, Width 60 u, Resistance 2.5 ohms
Evaporation of 40 mg of Indium

Run # 11a (10 gauss)

Pressure** (oil) (mm)	Pressure (Hg) (mm)	Temperature (°K)	DC current (ma)
	116.0	2.722	45.5
	82.0	2.533	56.0
	50.0	2.298	85.0
548	40.3	2.206	101.0
473	34.8	2.147	125.0
393	28.9	2.076	130.0
244	17.9	1.912	146.0

Run # 11b (30 gauss)

Pressure** (oil) (mm)	Pressure (Hg) (mm)	Temperature (°K)	DC current (ma)
	82.0	2.533	38.0
	49.0	2.289	57.0
540	39.7	2.200	70.0
464	34.1	2.139	94.0
366	26.9	2.049	100.0
186	13.7	1.830	123.0

Run # 11c (50 gauss)

Pressure** (oil) (mm)	Pressure (Hg) (mm)	Temperature (°K)	DC current (ma)
195	14.3	1.843	44.0

** Conversion factor of 13.6 applies.

thesH712
Magnetic field effects on critical curre
3 2768 002 06936 1
DUDLEY KNOX LIBRARY